

Death at watersheds: galaxy quenching in low-density environments

Maret Einasto¹, Rain Kipper¹, Peeter Tenjes¹, Jaan Einasto^{1,2,3}, Elmo Tempel^{1,2}, and Lauri Juhan Liivamägi¹

¹ Tartu Observatory, University of Tartu, Observatooriumi 1, 61602 Tõravere, Estonia

² Estonian Academy of Sciences, Kohtu 6, 10130 Tallinn, Estonia

³ ICRANet, Piazza della Repubblica 10, 65122 Pescara, Italy

Received / Accepted

ABSTRACT

Context. The evolution of galaxies is influenced by their local and global environment in the cosmic web. Galaxies with very old stellar populations (VO galaxies with $D_n(4000)$ index ≥ 1.75) mostly lie in the centres of galaxy clusters, where they evolve under the influence of processes characteristic of high-density cluster environments. However, VO galaxies have also been found in poor groups in global low-density environments between superclusters, which we call watershed regions.

Aims. Our aim is to analyse the properties of galaxies in various cosmic environments with a focus on VO galaxies in the watershed regions to understand their evolution, and the origin of the large-scale morphology–density relation.

Methods. We employ the Sloan Digital Sky Survey DR10 MAIN spectroscopic galaxy sample in the redshift range $0.009 \leq z \leq 0.200$ to calculate the luminosity–density field of galaxies, to determine groups and filaments in the galaxy distribution, and to obtain data on galaxy properties. The luminosity–density field with smoothing length $8 h^{-1}$ Mpc, D_8 , characterises the global environment of galaxies. We analyse the group and galaxy contents of regions with various D_8 thresholds. We divide groups into low- and high-luminosity groups based on the highest luminosity of groups in the watershed region, $L_{gr} \leq 15 \times 10^{10} h^{-2} L_\odot$. We compare the stellar masses, the concentration index, and the stellar velocity dispersions of quenched and star-forming galaxies among single galaxies, satellite galaxies, and the brightest group galaxies (BGGs) in various environments.

Results. We show that the global density is most strongly related to the richness of galaxy groups. Its influence on the overall star formation quenching in galaxies is less strong. Correlations between the morphological properties of galaxies and the global density field are the weakest. The watershed regions with $D_8 < 1$ are populated mostly by single galaxies, constituting 70 % of all galaxies there, and by low-luminosity groups. Still, approximately one-third of all galaxies in the watershed regions are VO galaxies. They have lower stellar masses, smaller stellar velocity dispersions, and stellar populations that are up to 2 Gyr younger than those of VO galaxies in other global environments. In higher density global environments ($D_8 > 1$), the morphological properties of galaxies are very similar. Differences in galaxy properties are the largest between satellites and BGGs in groups.

Conclusions. Our results suggest that galaxy evolution is determined by the birthplace of galaxies in the cosmic web, and mainly by internal processes which lead to the present-day properties of galaxies. This may explain the similarity of (VO) galaxies in extremely different environments.

Key words. large-scale structure of the Universe - galaxies: groups: general - galaxies: clusters: general

1. Introduction

Galaxies are systems of stars, gas, and dust held together by gravity within a dark matter halo. Broadly speaking, galaxies can be divided into two major classes based on their ability to form stars and their morphological and kinematic properties: actively star forming, blue, late-type galaxies, and passive, red, early-type galaxies (Strateva et al. 2001; Bell et al. 2017; Bluck et al. 2020a, 2022; Brownson et al. 2022; Driver et al. 2022). The ability of a galaxy to sustain star formation is determined by how well it can provide and cool gas. If the gas supply in a galaxy, which is governed by accretion, outflows, and mixing, is not sufficient to continue star formation, the star formation rate (SFR) drops and the galaxy becomes quenched or passive.

The processes that lead to star-formation quenching in galaxies can be divided into ‘internal’ and ‘external’ (Boselli & Gavazzi 2006; Paulino-Afonso et al. 2020). Internal processes, also referred to as mass quenching, depend first of all on the mass of the dark halo of a galaxy. Processes that blow

out galactic gas include stellar winds, supernova explosions, nuclear activity, active galactic nucleus (AGN) feedback, and so on (Matteucci et al. 2006; Croton et al. 2006; Henriques et al. 2019). These processes are more effective in massive galaxies (Contini et al. 2020) and at higher redshifts.

External processes that cause quenching of galaxies depend on the local environment of galaxies within clusters and/or groups (environmental quenching; see Pasquali et al. 2019; Werner et al. 2021, for definitions and references). External processes involve the stripping away of galactic gas by the ram pressure of the hot gas in a cluster or group (Gunn & Gott 1972; Yun et al. 2019), cold gas removal by viscous stripping (Nulsen 1982), starvation due to prevention of the arrival of fresh gas by removal of their feeding primordial filaments (Aragon Calvo et al. 2019; Maier et al. 2019), or harassment due to multiple high-speed mergers (Moore et al. 1996). External processes depend on environmental density, the orbital properties of galaxies, and also galaxy mass.

The formation and/or evolution of galaxies and the environment of galaxies are related (referred to as the nature-versus-

Send offprint requests to: Einasto, M.

nurture problem). While rich galaxy clusters and especially their central parts are mostly populated by early-type, red, quenched galaxies, late-type, blue, star-forming galaxies are preferentially found in poor groups, in the outskirts of clusters, or in the low-global-density environment. This is known as the morphological segregation of galaxies or the morphology–density relation, where ‘morphology’ denotes various properties of galaxies: their morphological type, star formation activity, colour, and so on. Einasto et al. (1974b), Dressler (1980), Postman & Geller (1984), Einasto & Einasto (1987), and Einasto (1991) demonstrated that the morphology–density relation extends from rich clusters to isolated galaxies in low-density environments. Jõeveer et al. (1978) and Einasto et al. (1980) showed that the central parts of the Perseus-Pisces supercluster are populated by early-type galaxies, while the fraction of late-type galaxies increases in the supercluster outskirts. The dependence of galaxy properties on environment was studied in detail by, for example, Goto et al. (2003), Gómez et al. (2003), Tempel et al. (2011), Park et al. (2007), Park & Choi (2009), Blanton & Moustakas (2009), Lietzen et al. (2012), and Alfaro et al. (2022). If galaxies stop forming stars in groups or filaments before falling into clusters, this is called preprocessing (Fujita 2004; McGee et al. 2009, 2014; Aragon Calvo et al. 2019; Džudžar et al. 2019; Castignani et al. 2022a,b). Even galaxies that do not belong to any group are more likely to be red and passive if they are located in superclusters (Einasto et al. 2007a; Lietzen et al. 2012; Einasto et al. 2014). This shows that global environment, which refers to scales larger than groups and clusters, may also be important in shaping galaxy properties.

In galaxy evolution, internal and external quenching processes often act together and it is not easy to decipher which one is dominating in different local and/or global environments. Understanding the formation of stars within galaxies and the end of star formation via the quenching processes is one of the most important unresolved problems in extragalactic astrophysics and cosmology. In this context, detailed studies of galaxies in various environments lead us to a better understanding of the formation and evolution of galaxies.

Most galaxies lie in groups of various richness and luminosity. In groups, galaxies can be divided into the brightest group galaxies (BGGs; often also called the central galaxies in groups) and satellite galaxies. There are also galaxies that do not belong to any group according to the criteria used to determine groups in galaxy distribution; we call these single galaxies. Single galaxies may represent various galaxy populations. They may be outer members of groups having closest group member galaxies that are too faint to be included in the given sample, in the Sloan Digital Sky Survey (SDSS) spectroscopic sample in our study. Single galaxies can also be isolated galaxies, that is, galaxies that do not have close bright galaxies according to certain criteria (Sulentic et al. 2006; Lacerna et al. 2016).

The large-scale distribution of galaxies can be described as the cosmic web: a network of galaxies and their groups and clusters, connected by galaxy filaments and separated by low-density regions with almost no visible galaxies. Systems of galaxies of various richness in the cosmic web represent global and local environments in which galaxies form and evolve. The present study focuses on the global environment of galaxies. We quantify global environment using the luminosity–density field. This field is calculated using a smoothing length $8 h^{-1}$ Mpc (in units of the mean luminosity–density, and denote as $D8$). In many studies, a threshold density of $D8 = 5$ is used to separate the largest overdensity regions, namely superclusters, from the underdense regions between them. Einasto et al. (2018a, 2019)

showed that superclusters occupy $\approx 1\%$ of the total SDSS sample volume, approximately 65% of the SDSS volume has very low global luminosity–density with $D8 < 1$, and in 90% of the SDSS volume, $D8 < 2$. Superclusters contain rich galaxy clusters and groups of galaxies connected by filaments. In underdense regions, galaxy groups and clusters are poor, and are typically connected by longer filaments than in superclusters (see Einasto et al. 2020, for details and references).

Simulations show that galaxies and their systems (groups and clusters) can form in the cosmic density field where large-scale density perturbations in combination with small-scale overdensities are sufficiently high (Peebles 2021; Einasto et al. 2011; Suhhonenko et al. 2011). In the underdense regions, galaxy groups are poor, and are too far apart to merge and form richer groups and clusters. Density fields and velocity fields are related; the velocities of galaxies are the lowest in the regions of lowest global density, where the formation of groups is also the slowest (Tempel et al. 2009; Einasto et al. 2021a). Einasto et al. (2020) found that while in the underdense region around the massive rich supercluster SCI A2142 —at a distance of $260 h^{-1}$ Mpc (with mass of $M \approx 4.3 \times 10^{15} h^{-1} M_{\odot}$ and more than 1000 member galaxies)—all groups are poor and do not show signatures of dynamical activity, even the poor groups in the supercluster have possibly started merging. Simulations show that in the regions of lowest global density where the global luminosity–density value is $D < 1.5$ (in units of mean luminosity–density), the sizes of haloes remain the same in a wide redshift interval, $\approx 1 h^{-1}$ Mpc, while in the regions of highest global luminosity–density (supercluster cores with $D8 > 7$), the sizes of haloes decrease by about five times during their evolution (Tempel et al. 2009). In underdense regions, the peculiar velocities of group-sized haloes have values below 500 km/s , and may be close to zero at the minima of the density field, while these velocities may have values higher than 500 km/s in superclusters (Nusser et al. 1991; Bahcall et al. 1994; Davis 1998).

In regions with increasingly high global density, groups are located closer together, and they can grow by merging and infall of galaxies or other groups (McGee et al. 2009; Muldrew et al. 2015; Ruiz-Lara et al. 2016). The richest clusters form at the locations of the highest density peaks (deep potential wells) where they attract matter from the surroundings more strongly than poor clusters found elsewhere. In the densest regions of the cosmic web (seeds of present-day rich clusters in supercluster cores), galaxies may have started to form earlier than elsewhere (Park et al. 2022). Groups that are found near rich clusters are also richer and more luminous than groups far from rich clusters, a phenomenon called environmental enhancement of poor groups (Einasto et al. 2003, 2005).

In accordance with earlier studies, Einasto et al. (2018b, 2021b) found that the inner, virialised parts of the richest clusters in superclusters are populated by galaxies with a $D_n(4000)$ index (ratio of the average flux densities in the bands $4000 - 4100\text{\AA}$ and $3850 - 3950\text{\AA}$) $D_n(4000) \geq 1.75$. Kauffmann et al. (2003) showed that such galaxies may have stellar populations with ages of at least 4 Gyr. Therefore, following Einasto et al. (2020), we refer to these galaxies with very old stellar populations as VO galaxies in order to distinguish them from galaxies that were quenched recently or are still forming stars. Somewhat unexpectedly, Einasto et al. (2020) found that VO galaxies are also common in poor groups and even among single galaxies in the underdense region around SCI A2142. There, 40% of galaxies in groups and one-third of single galaxies are VO galaxies. Isolated elliptical galaxies have also been found in filaments around

the Coma cluster in the Coma supercluster (Lacerna et al. 2016). Moreover, Einasto et al. (2020) showed that the properties of VO galaxies (morphology, concentration index, and other properties) are very similar across galaxy systems that are very different in terms of mass, from rich clusters in the supercluster to the poorest groups and single galaxies in global low-density environments.

The analyses in Einasto et al. (2020) and Lacerna et al. (2016) focused on the properties of a small sample of galaxies in the SCI A2142 and Coma superclusters and their environments. In the present study we aim to analyse the properties and environment of galaxies at various stages of star formation in a larger volume covered by the SDSS. One particular aim of our study is to search for VO galaxies in environments with the lowest global density, and to understand their properties.

To avoid mixing the influence of local (group) and global environment on galaxy properties, we analyse the properties of single galaxies, satellites, and brightest group galaxies in various global environments separately. Our study helps us to identify the main types of systems where galaxies are likely to be quenched. We aim to explore whether galaxy quenching occurs predominantly in rich clusters, which typically reside in global high-density environments, or also in poor groups and among single galaxies in the global low-density environment where conditions are very different from those in rich clusters.

We refer to the regions of lowest global luminosity–density as watersheds; that is, watersheds are the lowest-density parts of underdense regions between superclusters. We may expect the evolution of galaxies and groups in watershed regions to differ from that of galaxies in the high-density cores of rich clusters. Therefore, this study helps us to better understand the processes involved in galaxy evolution in various environments.

We compare the group and galaxy content, as well as the properties of galaxies in the watersheds with those in the higher global luminosity–density regions (higher-density parts of underdense regions and superclusters). Our first aim is to clarify whether or not VO galaxies also populate the watershed regions. Secondly, if we find such a population then we want to understand whether or not the properties of VO galaxies differ depending on whether they are located in watersheds or environments with higher global density. We also analyse whether there is a smooth change in galaxy properties with density or a sharp change in terms of galaxy and group properties at a certain threshold density that separates watersheds from regions of global higher density. In another series of comparisons, we investigate environmental trends in the properties of galaxies with young stellar populations with $D_n(4000) < 1.75$.

As in Einasto et al. (2020), we use data from the SDSS data release 10 (SDSS DR10) to analyse properties of galaxies and galaxy groups, with the following cosmological parameters: the Hubble parameter $H_0 = 100 h \text{ km s}^{-1} \text{ Mpc}^{-1}$, matter density $\Omega_m = 0.27$, parameter $h = 0.7$, and dark energy density $\Omega_\Lambda = 0.73$ (Komatsu et al. 2011).

2. Data on galaxies, groups, and their environment

We first describe how we determine the global environments of galaxies. For this task, we employ the luminosity–density field. In the luminosity–density field, the lowest density regions define the watersheds between superclusters, and the highest density regions correspond to superclusters. Global environment properties may be mixed with those caused by local environment. Examples of local environment are galaxy groups and single galaxies. Therefore we describe our group catalogue next. In groups,

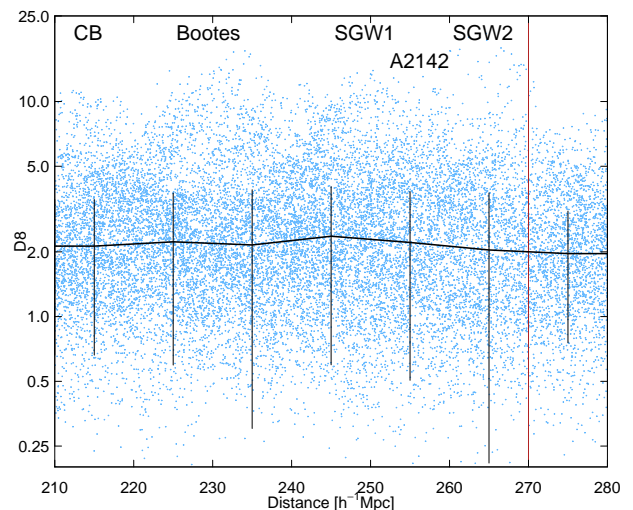


Fig. 1. Distribution of global luminosity density $D8$ around galaxies versus distance. The black line with error bars shows the median value of global luminosity density $D8$ at a given distance. We note that the logarithmic scale enhances low values of density and the associated errors. We mark several rich superclusters where $D8$ values are high. CB denotes the Corona Borealis supercluster, A2142 marks the supercluster SCL A2142, and SGW1 and SGW2 mark the locations of the two richest superclusters in the Sloan Great Wall. The dark red line shows the distance limit $270 h^{-1} \text{ Mpc}$ used to define our final sample of galaxies.

it is well known that the BGGs are more luminous and massive than satellite galaxies. Therefore, in order to avoid mixing large-scale effects and differences in galaxy properties within groups, we analyse single galaxies, satellites, and BGGs separately. Finally, we describe morphological properties of the galaxies analysed in this study, such as their stellar masses and other properties.

2.1. Global environment of galaxies: luminosity–density field

We use galaxy data from the SDSS DR10 MAIN spectroscopic galaxy sample with apparent Galactic extinction corrected r magnitudes $r \leq 17.77$ and redshifts $0.009 \leq z \leq 0.200$ (Aihara et al. 2011; Ahn et al. 2014). We calculated the absolute magnitudes of galaxies as

$$M_r = m_r - 25 - 5 \log_{10}(d_L) - K, \quad (1)$$

where d_L is the luminosity distance in units of $h^{-1} \text{ Mpc}$ and K is the $k+e$ -correction calculated as in Blanton & Roweis (2007) and Blanton et al. (2003) (see Tempel et al. 2014b, for details). As an order of magnitude reference, the limiting magnitude $r = 17.77$ at $z = 0.1$ corresponds to the stellar mass $M^* \simeq 1.8 \times 10^{10} M_\odot$, which is twice the stellar mass of large satellites in the Local Group, the Large Magellanic Cloud, or the Triangulum Nebula.

We characterise the global environment of galaxies using the luminosity–density field (Liivamägi et al. 2012). This field is calculated using a smoothing kernel based on the B_3 spline function:

$$B_3(x) = \frac{|x-2|^3 - 4|x-1|^3 + 6|x|^3 - 4|x+1|^3 + |x+2|^3}{12}. \quad (2)$$

The details of the calculation of density field using a B_3 spline kernel can be found in Einasto et al. (2007b); Tempel et al. (2014b). We use a smoothing length of $8 h^{-1} \text{ Mpc}$ to define the

global luminosity–density field, and denote global luminosity–density as $D8$. Luminosity–density values are expressed in units of mean luminosity density, $\ell_{\text{mean}} = 1.65 \cdot 10^{-2} \frac{10^{10} h^{-2} L_{\odot}}{(h^{-1} \text{Mpc})^3}$. In the luminosity–density field, superclusters can be defined as the connected volumes above a threshold density of $D8 = 5.0$ (as in e.g. Liivamägi et al. 2012; Einasto et al. 2014, 2020). In the following analysis, we use a series of global luminosity–density $D8$ intervals to study the trends in galaxy and group properties with global density. The lowest global density interval corresponds to low-density watershed regions between superclusters, and the highest global densities ($D8 \geq 5$) correspond to superclusters. The global density regions with intermediate densities represent medium-density regions around superclusters.

We also employ luminosity–density field with smoothing length $1 h^{-1} \text{Mpc}$ to define local luminosity–density field around single galaxies, denoted as $D1$. For galaxies in groups, local environment is defined by group membership, which we define in the following subsection.

In studies of environmental trends of galaxy properties, density is typically defined by N th nearest neighbours (see e.g. Blanton & Moustakas 2009, for a review and references). For our purposes, the use of the luminosity–density field is preferable because with this approach we can distinguish between various global environments.

2.2. Group data

The majority of galaxies belong to groups of different richness, from galaxy pairs to the richest clusters. To take this into account we obtained data on group membership for galaxies from group catalogues by Tempel et al. (2012, 2014b,a). These catalogues are based on the SDSS DR10 MAIN spectroscopic galaxy sample described in the previous section. Catalogues of galaxy groups are available at the CDS¹.

Galaxy groups in these catalogues were determined using the friends-of-friends cluster analysis method (Zeldovich et al. 1982; Huchra & Geller 1982), where a galaxy is considered a member of a group if it lies less than linking length from at least one group member galaxy. In a flux-limited sample, the density of galaxies slowly decreases with distance. To properly take this selection effect into account when a group catalogue is constructed, the linking length is re-scaled with distance, calibrating the scaling relation by observed groups. As a result, the maximum sizes in the sky projection and the velocity dispersions of the groups are similar at all distances. The redshift-space distortions (also known as Fingers of God) for groups were suppressed, as described in detail in Tempel et al. (2014b).

In the Tempel et al. (2014b) group catalogue, the luminosities of groups L_{gr} are calculated using r -band luminosities of group member galaxies, corrected for the missing (unobserved) galaxies at a distance of a given group. In groups, it is well known that the BGGs differ in their properties from satellite galaxies. Therefore, in order to avoid mixing large-scale effects and differences in galaxy properties within groups, we distinguish between satellite galaxies and BGGs in our analysis.

There are galaxies in our sample that are not members of any group. We call these single galaxies and analyse them separately. Single galaxies may also be the brightest galaxies of groups of which the other members are too faint to be included in the SDSS MAIN spectroscopic sample. They may also be outer satellites of groups, connected to the other group member galaxies by faint galaxies that are not in the sample. Single galaxies may belong

to samples of isolated galaxies if the magnitude difference between the galaxy and its brightest satellites and the distance to the nearest bright galaxy are large enough to satisfy the conditions to be included in such a sample; as described, for example, in Sulentic et al. (2006) and in Lacerna et al. (2016). Isolated galaxies may be hypergalaxy-type systems in which giant galaxies are surrounded by dwarf satellites (Einasto et al. 1974a).

2.3. Selection effects and final sample

The SDSS MAIN sample covers various global density environments from voids to superclusters. At distances shorter than $\approx 200 h^{-1} \text{Mpc}$ the SDSS sample is narrow, and it crosses an underdense region between the Hercules supercluster and the Bootes and the Corona Borealis superclusters. At distances greater than $270 h^{-1} \text{Mpc}$ there is a large underdense region without rich superclusters. The distance interval $210 - 270 h^{-1} \text{Mpc}$ covers the region with rich and very rich superclusters, such as the Sloan Great Wall, the Corona Borealis supercluster, the Bootes supercluster, and SCI A2142, and the underdense regions between them. More details about these structures can be found, for example, in Einasto et al. (2012a) and in Einasto et al. (2014). To minimise distance-dependent selection effects in our study, we need to have a variety of global environments at the same distances. Therefore, we use the distance range $210 - 270 h^{-1} \text{Mpc}$ which satisfies this condition. Figure 1 shows the luminosity–density $D8$ around galaxies versus distance. Several peaks in the density distribution can be seen at the location of rich superclusters. The median value of global luminosity–density in this distance interval is $D8_{\text{med}} \approx 2.1$. Figure 1 shows that the median value of $D8$ is almost unchanged with distance, but the scatter of densities at a given distance interval is large. This is related to the presence of both over- and underdensity structures at a given distance interval.

As we use a flux-limited (apparent magnitude limited) galaxy sample to construct our group catalogue, the group luminosities and richness are affected by distance-dependent selection effects. This is shown in Fig. 2, where we plot group luminosities versus their distance and group richness versus group luminosity in a distance interval of $210 - 270 h^{-1} \text{Mpc}$ (redshift range $0.07 \leq z \leq 0.100$). We highlight groups in the lowest global density environment with $D8 \leq 1$. The flux-limited nature of our galaxy sample also affects group luminosities; low-luminosity groups are absent among more distant groups. The right panel of Fig. 2 shows that this selection affects mostly galaxy pairs in all global density environments. To minimise this effect, we exclude groups with luminosity limit $L_{gr} < 1.8 \times 10^{10} h^{-2} L_{\odot}$ from a complete sample of groups (mostly galaxy pairs).

Figure 2 shows that in the lowest global density region, $D8 \leq 1$, all groups are poor, with $N_{gal} \leq 9$ and of low luminosity, $L_{gr} \leq 15 \times 10^{10} h^{-2} L_{\odot}$ (only one group with four galaxies in this global density interval has luminosity $L_{gr} > 15 \times 10^{10} h^{-2} L_{\odot}$). As the group richness is more strongly affected by selection effects, in what follows we use group luminosities to define samples of low-luminosity groups (LLGs) and high-luminosity groups (HLGs). Low-luminosity groups have group luminosity limits $1.8 \times 10^{10} h^{-2} L_{\odot} \leq L_{gr} \leq 15 \times 10^{10} h^{-2} L_{\odot}$, while HLGs have $L_{gr} > 15 \times 10^{10} h^{-2} L_{\odot}$. These limits are shown in Fig. 2. For a statistical comparison of galaxy properties, we apply an absolute magnitude limit of $M_r = -19.6 \text{mag}$. This limit corresponds to a volume-limited sample in the distance interval used in our

¹ cdsarc.u-strasbg.fr

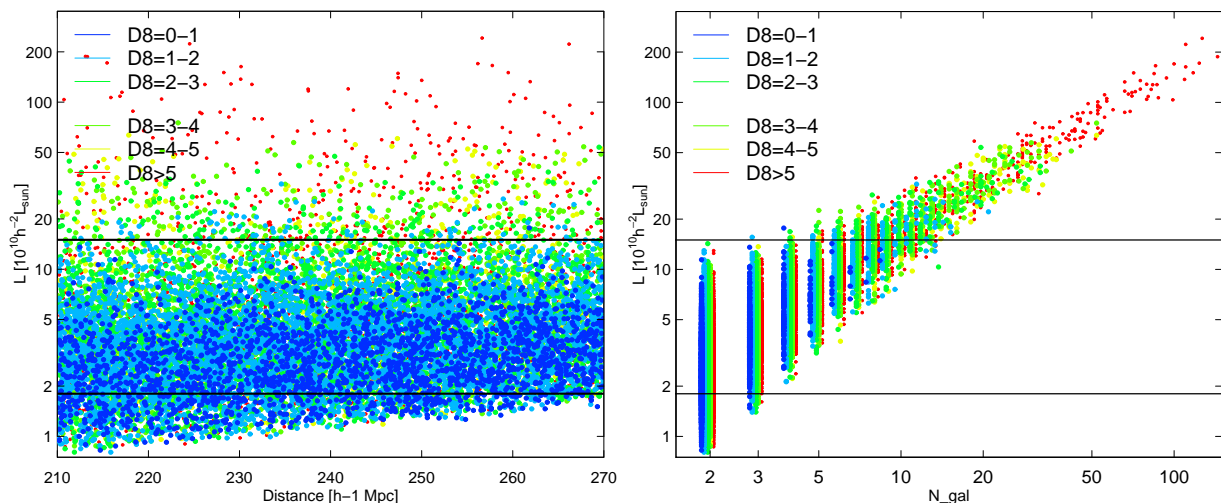


Fig. 2. Total luminosity of groups versus group distances (left panel) and group richness (right panel). In the right panel, group richness is shifted to avoid overlapping, which is especially strong for groups with up to five galaxies.

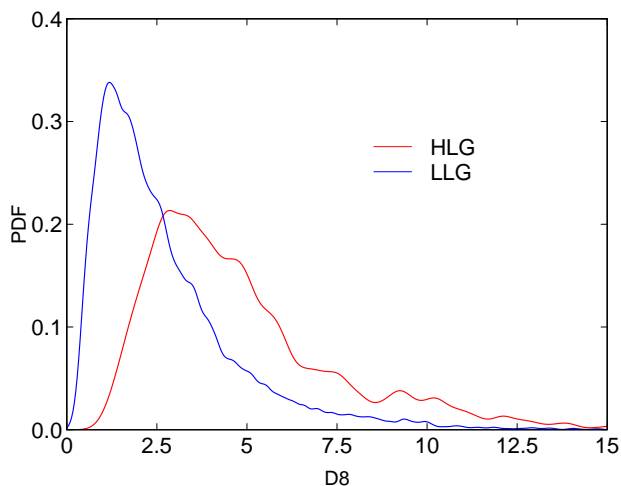


Fig. 3. Distribution of global densities $D8$ at the location of HLGs (red line) and LLGs (blue line).

study. In total, within the distance interval $210 - 270 h^{-1}$ Mpc and given luminosity limits, we have data for 81527 galaxies.

Figure 3 shows the distribution of global densities $D8$ at the locations of groups. From this figure, we see that although LLGs are present in all global density environments, and HLGs are present everywhere except the lowest global density region with $D8 \leq 1$, the distribution of global densities at their location is different. LLGs preferentially occupy regions outside superclusters ($D8 < 5$), while over 50% of HLGs lie in superclusters. High-density cores of superclusters with $D8 > 8$ are populated mostly by HLGs (mostly rich clusters). The number of such groups in our sample is small, and we do not analyse them separately.

We show the sky distribution of groups from our sample in Fig. 4 where we show groups in a $20 h^{-1}$ Mpc thin slice in the distance range of $210 - 230 h^{-1}$ Mpc which covers the regions of two superclusters (part of the Corona Borealis supercluster at $R.A. = 207^\circ$ and $Dec. = +28^\circ$, and the Bootes supercluster at $R.A. = 230^\circ$ and $Dec. = +27^\circ$), and a low-density region between and around them. The locations of these superclusters are also marked in Fig. 1. Figure 4 shows how groups in the low-global-density region separate superclusters, which occupy only 1% of

the total volume. Groups appear to form filaments, and richer groups lie at the crossings of these filaments.

2.4. Morphological data of galaxies

To compare galaxy samples of various classes we use galaxy morphological data: $D_n(4000)$ index, SFR, stellar masses M^* , stellar velocity dispersion σ^* , and concentration index C . Data on galaxy properties for our study are taken from the SDSS DR10 web page². Below, we list the data for the galaxies used in this paper.

The data on $D_n(4000)$ index are from the MPA-JHU spectroscopic catalogue (Tremonti et al. 2004; Brinchmann et al. 2004). The $D_n(4000)$ index is the ratio of the average flux densities in the band $4000 - 4100 \text{ \AA}$ to those in the band $3850 - 3950 \text{ \AA}$, and is correlated with the time passed since the most recent star formation event in a galaxy (Kauffmann et al. 2003). This index can be used as proxy for the ages of the stellar populations of galaxies, and their SFRs. We use the $D_n(4000)$ index of galaxies as calculated in Balogh et al. (1999).

Data on stellar masses M^* and SFRs are taken from the MPA-JHU spectroscopic catalogue (Tremonti et al. 2004; Brinchmann et al. 2004). In this catalogue, the properties of galaxies are calculated using the stellar population synthesis models and fitting SDSS photometry and spectra with Bruzual & Charlot (2003) models. The stellar masses of galaxies are calculated as described in Kauffmann et al. (2003). The SFRs were computed using the photometry and emission lines as described by Brinchmann et al. (2004) and Salim et al. (2007). Stellar velocity dispersions of galaxies, σ^* , are calculated by fitting galaxy spectra using publicly available codes, namely the Penalized PiXel Fitting code (pPXF, Cappellari & Emsellem 2004) and the Gas and Absorption Line Fitting code (GANDALF, Sarzi et al. 2006). The concentration index of galaxies C is calculated as the ratio of the Petrosian radii R_{50} and R_{90} : $C = R_{50}/R_{90}$, which themselves are defined as the radii containing 50% and 90% of the Petrosian flux of a galaxy, respectively (Blanton et al. 2001; Yasuda et al. 2001).

We divide galaxies into those with old and young stellar populations using the $D_n(4000)$ index. Earlier studies showed that the central, virialised parts of galaxy clusters (ancient in-

² <http://skyserver.sdss3.org/dr10/en/help/browser/browser.aspx>

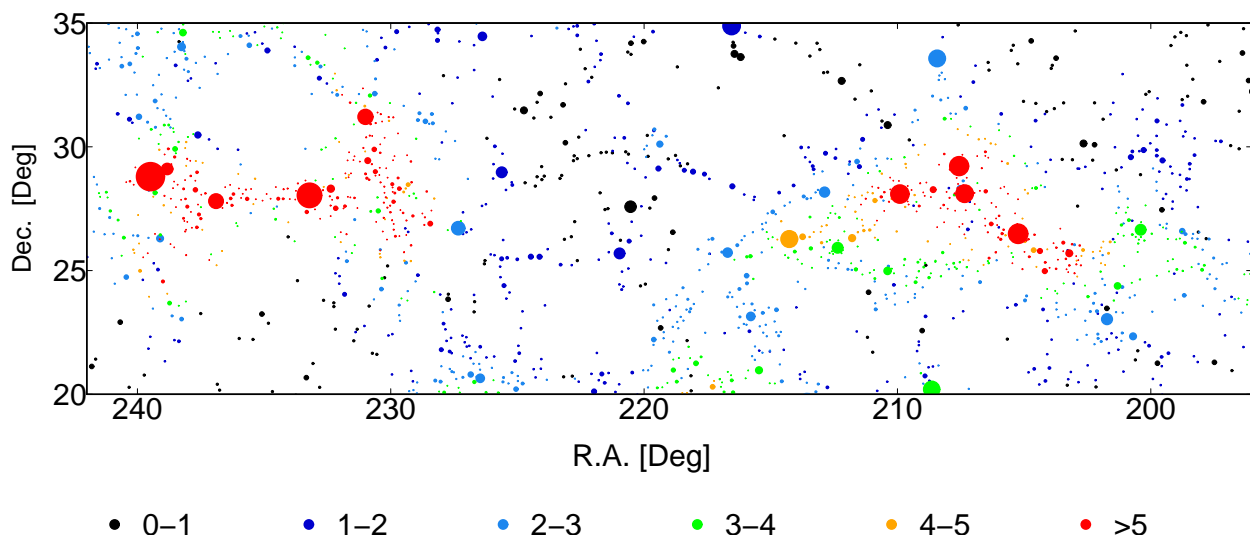


Fig. 4. Distribution of groups in the sky plane in a slice of thickness of $20 h^{-1}$ Mpc at a distance interval $210 - 230 h^{-1}$ Mpc which partly covers the Corona Borealis supercluster at $R.A. = 230^\circ$ and $Dec. = +27^\circ$, and the Bootes supercluster at $R.A. = 207^\circ$ and $Dec. = +28^\circ$, and the low-density region between and around them. The sizes of the circles are proportional to the richness of the groups. We only plot the location of the brightest galaxy of any given group. Colours code the limits of global density D_8 in the environment of galaxies.

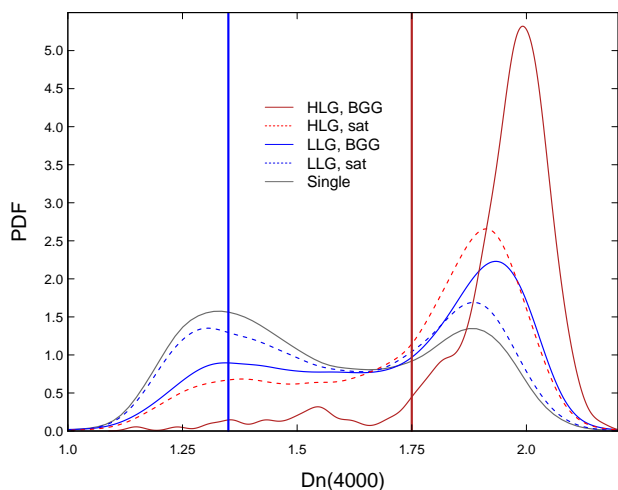


Fig. 5. Distribution of $D_n(4000)$ index for single galaxies (solid grey line), and for satellite galaxies (dashed lines) and BGGs (solid lines) in LLGs (blue lines) and HLGs (red lines). Vertical lines show the values of $D_n(4000)$ index $D_n(4000) = 1.35$ ($D_n(4000)$ limit for galaxies with very young stellar populations), and $D_n(4000) = 1.75$ (limit for VO galaxies with $D_n(4000) \geq 1.75$, see text).

fall regions in the projected phase space diagrams) are populated mostly by galaxies with $D_n(4000) \geq 1.75$ (Einasto et al. 2018b, 2020, 2021b). According to Kauffmann et al. (2003), the value $D_n(4000) = 1.75$ corresponds to a mean age of about 4 Gyr (for Solar metallicity) or older (for lower metallicities). Values $D_n(4000) > 2.0$ approximately correspond to a stellar age of 10 Gyr (Kauffmann et al. 2003), that is, such galaxies stopped forming stars at redshifts $z \approx 1.5 - 2$. In the present study, we apply the limit $D_n(4000) = 1.75$, above which we define galaxies as having very old stellar populations (VO galaxies).

To separate galaxies with old and young stellar populations the limit $D_n(4000) = 1.55$ can be used; this limit approximately corresponds to a mean age of stellar populations of a galaxy about 1.5 Gyr (Kauffmann et al. 2003). Galaxies with $D_n(4000) > 1.55$ are often referred to as passive or red

and dead. We use the term VO to emphasise the use of a higher $D_n(4000)$ index value, $D_n(4000) = 1.75$. Below the value $D_n(4000) = 1.35$, galaxies are considered to have very young stellar populations with a mean age of approximately 0.6 Gyr only (Kauffmann et al. 2003). Einasto et al. (2020) and Einasto et al. (2021b) showed that in the $D_n(4000)$ –stellar mass plot, galaxies with $D_n(4000)$ index in the interval of $1.35 < D_n(4000) \leq 1.75$ belong to mixed populations, containing quenched galaxies with no active star formation, red and blue star forming galaxies, and recently quenched galaxies (those with young stellar populations but with no active star formation). We analysed the trends with global density for each of these populations, and because these were similar for these populations, we show the results for them taken together. Therefore, in what follows, we analyse two populations of galaxies: VO galaxies with $D_n(4000) \geq 1.75$, and all other galaxies with $D_n(4000) < 1.75$ taken together as galaxies with young stellar populations (hereafter YS galaxies).

Figure 5 shows the distribution of the $D_n(4000)$ index for single galaxies, and for satellites galaxies and BGGs in low- and high-luminosity groups. This figure already shows important difference between BGGs of HLGs, and all other galaxy classes: almost all of them are VO galaxies, and there are very few YS galaxies among them. The percentage of VO galaxies among other galaxy classes increases from 31% of single galaxies to 61% of satellites of HLGs; see Table 1.

The $D_n(4000)$ index can be used as an indicator of the SFRs in galaxies. We also analyse the SFR of galaxies directly. Galaxies with $\log \text{SFR} \geq -0.5$ are considered as star forming, and those with $\log \text{SFR} < -0.5$ are passive, quenched galaxies.

Earlier studies showed that the concentration index of galaxies C is related to the galaxy structure parameters. Early-type elliptical galaxies have lower values of C than disk-dominated late-type galaxies (Graham et al. 2005; Einasto et al. 2020). Strateva et al. (2001) showed that the value $C \approx 0.38$ separates early- from late-type galaxies.

The stellar velocity dispersion of galaxies, σ^* , also correlates with other galaxy properties. Typically, star forming galaxies (i.e. the YS galaxies in the present study) have a lower stellar velocity dispersion σ^* than quiescent galaxies (i.e. the VO galax-

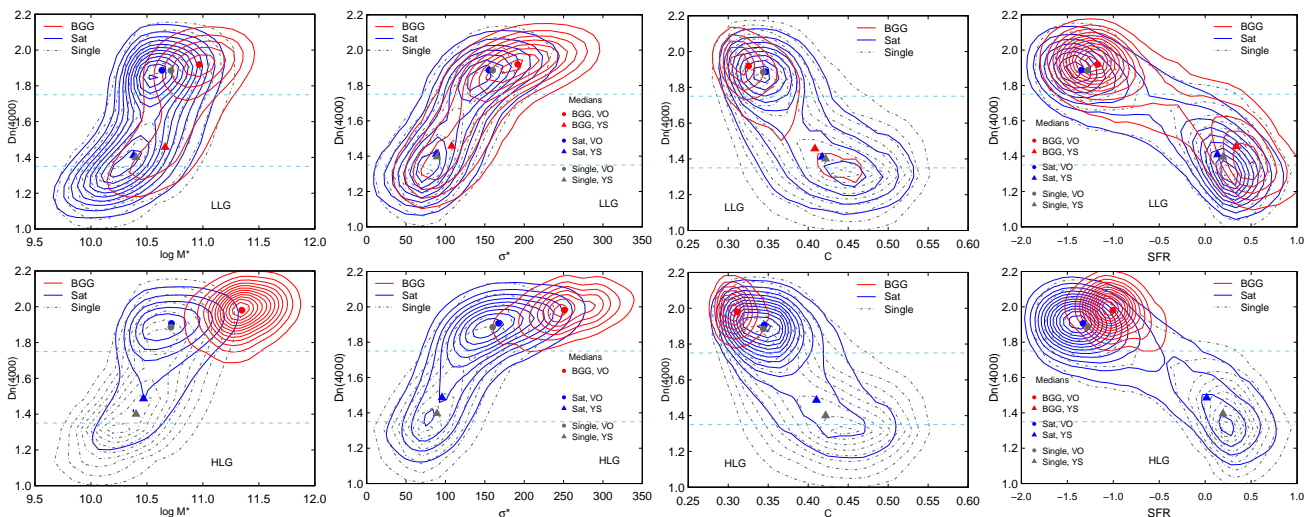


Fig. 6. Stellar mass $\log M^*$ (leftmost panels), stellar velocity dispersions σ^* (left central panels), concentration index of galaxies C (right central panels), and \log SFR (rightmost panels) versus $D_n(4000)$ index for galaxies in LLGs (upper row), and in HLGs (lower row). Filled circles and triangles show median values of galaxy properties for VO (circles) and YS (triangles) galaxies, as described in the legend in σ^* and \log SFR panels. Horizontal lines show the values of $D_n(4000)$ index $D_n(4000) = 1.35$ and $D_n(4000) = 1.75$.

ies here). The stellar velocity dispersion of a galaxy correlates with the mass of its supermassive black hole (see Bezanson et al. 2012; Einasto et al. 2020, for details and references). Observations show that at the high end of the stellar velocity dispersion, $\sigma^* > 300$ km/s, σ^* has changed very little since $z \approx 1.5$, suggesting that the galaxies with the most massive black holes have almost not changed over the last 10 Gyr (Bezanson et al. 2012).

2.5. Abbreviations

To make the paper easier to follow, below we list some of the abbreviations introduced above. They are used in our paper to characterise group membership and the star formation properties of galaxies.

- VO = galaxy with very old stellar populations with $D_n(4000) \geq 1.75$;
- YS = young, star-forming galaxies with $D_n(4000) < 1.75$ (this is mixed populations, and includes quenched galaxies with no active star formation, red and blue star forming galaxies, and recently quenched galaxies);
- BGG = brightest group galaxies;
- Sat = satellite galaxies in groups;
- Single = galaxies which do not belong to any group;
- LLGs = low-luminosity groups with luminosity limits $1.8 \times 10^{10} h^{-2} L_\odot \leq L_{gr} \leq 15 \times 10^{10} h^{-2} L_\odot$;
- HLGs = high-luminosity groups with $L_{gr} > 15 \times 10^{10} h^{-2} L_\odot$;
- CWD = cosmic web detachment.

3. Results

In this section, we present our main results. We start with our analysis of the morphological data of single galaxies, satellites, and BGGs. Thereafter, we analyse galaxy and group content in various global density environments using data on the group membership of galaxies and the $D_n(4000)$ index. The section ends with a comparison of other morphological properties of galaxies with old and young stellar populations in various global density regions.

3.1. Morphological properties of single galaxies, satellites, and BGGs

We plot stellar mass $\log M^*$, stellar velocity dispersion σ^* , SFR , and C of galaxies versus $D_n(4000)$ index in Fig. 6. In each panel, we plot satellite galaxies, BGGs, and single galaxies separately. Single galaxies in both rows are the same, they are plotted for comparison. Figure 6 also shows $D_n(4000)$ index limits $D_n(4000) = 1.75$, and $D_n(4000) = 1.35$. Table 2 presents the median values of galaxy properties in each population. Errors are very small, typically less than 0.1 %, and are not given so as to avoid overcrowding the table.

A bimodality in galaxy morphological properties is clearly seen in Fig. 6 as a ‘red cloud’ above $D_n(4000) \approx 1.55$ and $\log SFR < -0.5$, and ‘blue cloud’ below this limit, around $\log SFR \geq -0.5$. The $D_n(4000)$ index interval $1.35 - 1.75$ (‘green valley’) covers galaxies from mixed populations, including galaxies in transformation (red star forming galaxies at the high-stellar-mass end in this $D_n(4000)$ interval, and recently quenched galaxies at the low-stellar-mass end). These galaxies are mostly of late type, although there are also early-type galaxies among them, as suggested by their concentration index in the right panels. This agrees with the recent results of Quilley & de Lapparent (2022), who show that galaxies in the green valley are mostly of late type. We also note that a small fraction of galaxies have $D_n(4000) \geq 1.75$ and $\log SFR \geq -0.5$. These are VO galaxies that are still forming stars. Such galaxies form 2% of all galaxy populations (single galaxies, and galaxies in LLGs and HLGs). This very small percentage tells us that the high value of $D_n(4000)$ index, $D_n(4000) = 1.75$, can be used to separate quenched and star forming galaxies.

Let us now analyse what Fig. 6 tells us about galaxy populations in LLGs (upper row) and single galaxies. To begin with, we reiterate the fact that BGGs were selected on the basis of galaxy luminosity, being the most luminous galaxies in a group. In what follows, we compare other properties of galaxies. Figure 6 shows that in the case of both the red and blue cloud galaxies, BGGs occupy areas of higher stellar mass and velocity dispersion. The concentration indices of BGGs are somewhat lower, meaning that their morphological types are slightly earlier compared to satellites and single galaxies. BGGs avoid the area of

lowest stellar mass in the left panel. BGGs in LLGs also avoid the lowest values of $D_n(4000)$ index although some of them have higher values of SFRs than LLG satellites or single galaxies. The median values for BGGs in all panels indicate the same trend. At the same time, the properties of satellites and single galaxies are very similar. As mentioned above, single galaxies can be the BGGs of faint groups of which the other member galaxies are too faint to be included in the SDSS spectroscopic sample. They can also be outer satellites of groups, which could explain the similarity of their properties. We discuss the possible connection between single galaxies and satellites further in Sect. 4.2.

In HLGs (lower row in Fig. 6), BGGs clearly differ in their star formation properties from other galaxies. More than 90% of these are VO galaxies with $D_n(4000) \geq 1.75$, although even among these approximately 2% of galaxies have $\log \text{SFR} \geq -0.5$. HLG BGGs have much higher stellar masses than satellite galaxies, and also higher stellar velocity distributions and lower concentration indexes than satellites galaxies. According to concentration index, they have clearly earlier morphological types than satellites or single galaxies. Galaxies with $\sigma^* > 300$ km/s in our sample are all BGGs of HLGs. These galaxies have $D_n(4000) > 1.85$, and therefore both their $D_n(4000)$ index and σ^* values suggest that they stopped forming stars and have not changed much over the last 10 Gyr.

Figure 6 reveals that the properties of satellite galaxies in HLGs with $D_n(4000) \geq 1.75$ are close to those of VO single galaxies, and the corresponding median values of galaxy properties almost overlap. At the lower $D_n(4000)$ index end (YS population), satellites of HLGs have, on average, higher stellar masses and stellar velocity dispersions and lower concentration index than single galaxies. HLG satellites also avoid the lowest end of the $D_n(4000)$ index values, meaning that their stellar populations are, on average, older than the stellar populations of YS single galaxies. Nevertheless, it is interesting that the differences between the properties of HLG satellites and single galaxies are rather small.

Our comparison of the galaxy parameters of single galaxies, satellites, and BGGs of LLGs and HLGs in Fig. 6 suggests that galaxy population type is the major parameter determining the quenching status of galaxies. The difference between the fractions of BGGs and satellite galaxies is the largest in HLGs, and is also fairly large in LLGs, as seen in Table 1.

According to Tempel et al. (2014a), approximately 35%–40% of all galaxies are members of filaments. To find the fraction of the galaxies in our sample that belong to filaments, we used data on galaxy filaments from filament catalogues by Tempel et al. (2014a) and Tempel et al. (2016). Our preliminary analysis shows that approximately 50% of the galaxies in LLGs are filament members, compared to 40% of those in HLGs. A comparison of the properties of the galaxies found in and outside of filaments shows that approximately 25% of filament member galaxies have $D_n(4000) \geq 1.75$. Comparison with the percentages given in Table 2 shows that the percentages of VO galaxies in filaments are lower than the percentages of VO galaxies among any population in Table 2. This difference may be related to the fact that only some groups lie in filaments, and the percentage of galaxies in groups with $D_n(4000) \geq 1.75$ is higher than the same percentage of galaxies not in groups. A detailed analysis of galaxy quenching in filaments is beyond the scope of this paper, and merits a separate study.

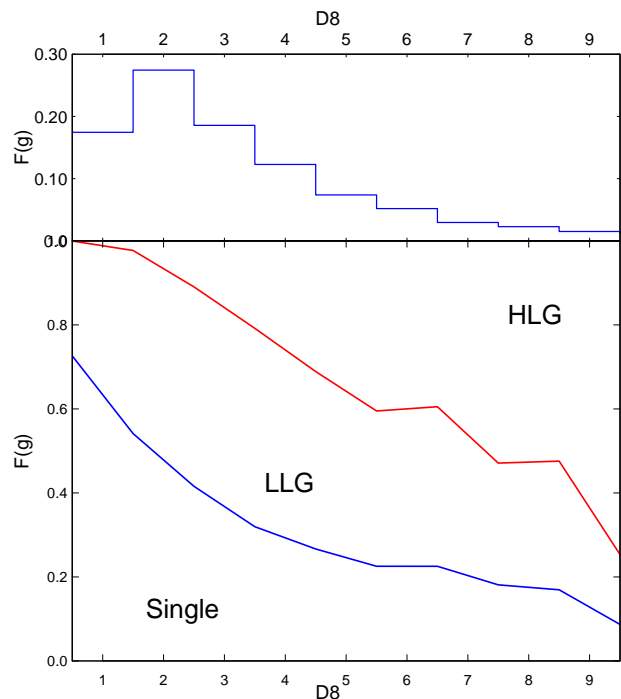


Fig. 7. Percentage of galaxies $F(g)$ from all galaxies in various global density $D8$ intervals (upper panel), and the percentage of single galaxies, LLG members, and HLG members in various global density $D8$ intervals (lower panel).

3.2. Group and galaxy content of various global environments

Now we analyse the overall group and galaxy content of various global density environments. We first show the percentage of galaxies from total sample, and the percentages of single galaxies and member galaxies of LLGs and HLGs in various global density environments (Fig. 7, upper and lower panels). These percentages are presented also in Table 1.

First, Table 1 and Fig. 7 show that the galaxy and group populations change significantly with global density. Single galaxies and poor, low-luminosity groups can be found everywhere in the cosmic web, from the regions of lowest global density to superclusters. Figure 2 demonstrates that, in accordance with the general understanding of the formation of groups in the cosmic web, groups in the lowest global density regions are poor and of low luminosity. Figure 7 reveals that in watersheds, even the formation of poor groups is suppressed; watersheds are mostly populated by single galaxies (73% of all galaxies). LLGs host 27% of all galaxies here. At higher global densities, at first the percentage of galaxies in LLGs increases and that of single galaxies decreases. In global density interval $1 < D8 < 2$, the percentage of single galaxies drops to 54%, and 44% of galaxies are members of LLGs. Only 2% of all galaxies in this density interval reside in HLGs. Then, as the global density increases, the percentage of galaxies in HLGs starts to grow. In the environments of highest global density, more than 50% of all galaxies lie in HLGs, and only 17% of galaxies are single.

In order to investigate the distribution of galaxies with different star formation properties among galaxies in a given global density interval, we show in Fig. 8 the percentage of galaxies from different $D_n(4000)$ index ranges versus global density $D8$. Here, we also show the percentage of galaxies with $D_n(4000) > 2.0$, which approximately corresponds to an age

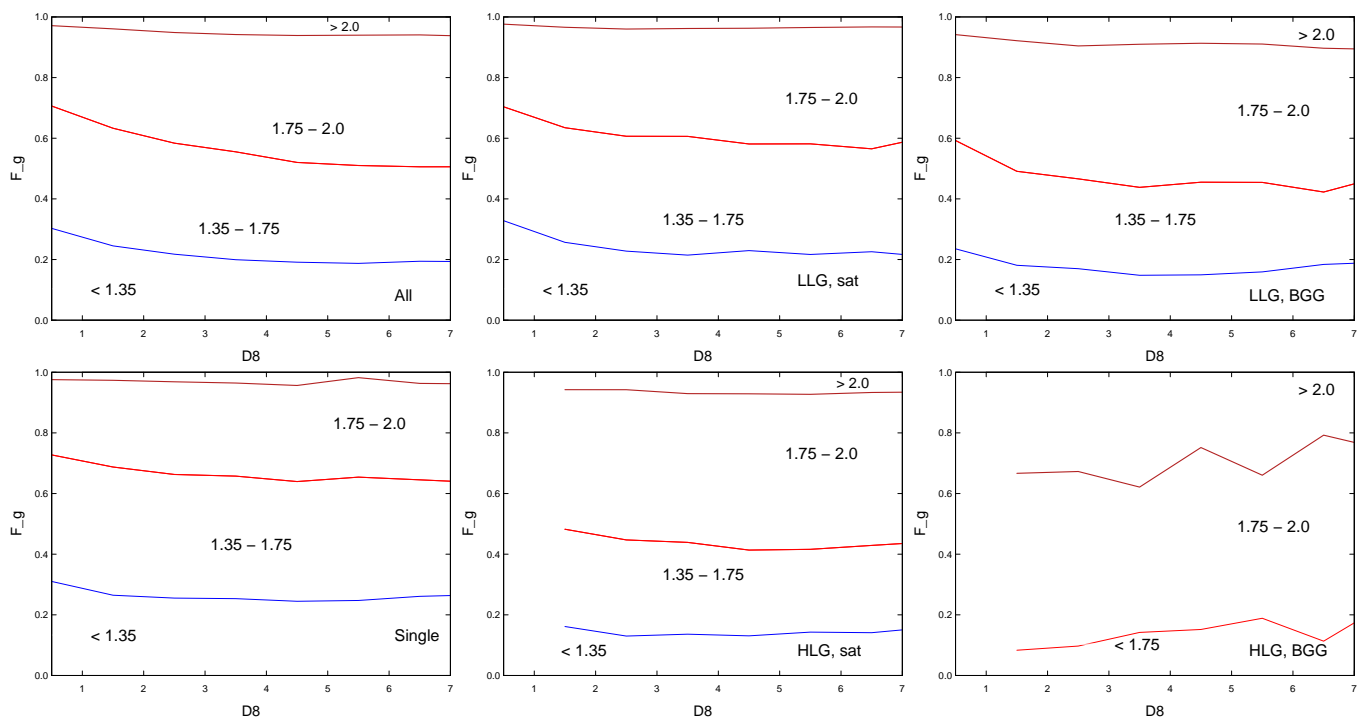


Fig. 8. Galaxy content of various global density $D8$ regions according to the $D_n(4000)$ index in the following intervals: $D_n(4000) \leq 1.35$, $1.35 < D_n(4000) \leq 1.75$, $1.75 < D_n(4000) \leq 2.0$, and $D_n(4000) > 2.0$. Upper left panel: All galaxies. Upper middle panel: LLG satellite galaxies. Upper right panel: LLG BGGs. Lower left panel: Single galaxies. Lower middle panel: HLG satellite galaxies. Lower right panel: HLG BGGs.

Table 1. Galaxy populations in various global density intervals.

(1)	(2)	(3)	(4)	(5)	(6)	(7)	(8)	(9)	(10)	(11)	(12)
D8 limits	N_{gal}	F_{gal}	F_1	F_{LLG}	F_{HLG}	F_{all}^{VO}	F_1^{VO}	F_{LLG}^{VO}	Sat BGG	Sat	BGG
< 1	14226	0.17	0.73	0.27	0	0.30	0.27	0.30	0.42	0	0
1 – 2	22378	0.27	0.54	0.44	0.02	0.37	0.31	0.37	0.53	0.53	0.92
2 – 3	15135	0.19	0.42	0.47	0.11	0.43	0.33	0.40	0.56	0.57	0.93
3 – 4	10014	0.12	0.32	0.47	0.21	0.46	0.34	0.39	0.59	0.58	0.91
4 – 5	6025	0.07	0.27	0.42	0.31	0.50	0.35	0.41	0.57	0.60	0.95
> 5	13749	0.17	0.17	0.30	0.53	0.55	0.36	0.42	0.59	0.62	0.92

Notes. Columns are as follows: (1): Interval of global luminosity density $D8$, in units of mean density (see text); (2): Number of galaxies in the given density interval (3): Percentage of galaxies in the given density interval among all galaxies; (4–6): Percentage of single galaxies F_1 , and percentages of galaxies in low- and high- luminosity groups (F_{LLG} and F_{HLG}) in the given density interval; (7): percentage of VO galaxies with $D_n(4000) \geq 1.75$ among all galaxies in the given density interval; (8): percentage of VO galaxies with $D_n(4000) \geq 1.75$ among single galaxies in the given density interval; (9–10): percentage of VO galaxies among satellite galaxies and BGGs of low-luminosity groups (LLGs) in the given density interval; (11–12): percentage of VO galaxies among satellite galaxies and BGGs of low-luminosity groups (HLGs) in the given density interval.

of 10 Gyr for the stellar populations therein (Kauffmann et al. 2003). This suggest that these galaxies may have stopped forming stars at redshifts $z \approx 1.5 - 2$. We mention that less than 0.1 % of these galaxies may still be forming stars, as they have $\log SFR \geq -0.5$. Observations have found quenched galaxies even at redshifts as high as $z = 3.37$ (McConachie et al. 2022), and therefore the high fraction of quenched BGGs and other galaxies at redshifts $z \approx 1.5 - 2$ does not come as a surprise. Additionally, Fig. 9 shows the distribution of $D_n(4000)$ index for single galaxies, satellites, and BGGs in various global density environments. The percentages of VO galaxies among galaxies according to their group membership are given in Table 1.

Figures 8 and 9 and Table 1 show that VO galaxies are found in environments of all global densities. Even in the watershed re-

gion, 30% of all galaxies, and 27% of single galaxies have very old stellar populations. In contrast, in the highest global density regions (superclusters), 55 % of all galaxies are with very old stellar populations. In all global density intervals, the percentage of VO galaxies is lower in LLGs than in HLGs (both among satellites and BGGs, Table 1). Among galaxies in LLGs, 29% of satellite galaxies and 40% of BGGs are VO galaxies in the $D8 < 1$ region. These percentages increase up to 40% and 60% in higher global density regions. Interestingly, the percentage of VO galaxies among BGGs of LLGs is almost unchanged over a wide global density range, $D8 > 2$, while among satellite galaxies of LLGs there is an increasing percentage of VO galaxies with increasing global density. It is also interesting to see that among single galaxies, which are the least affected by

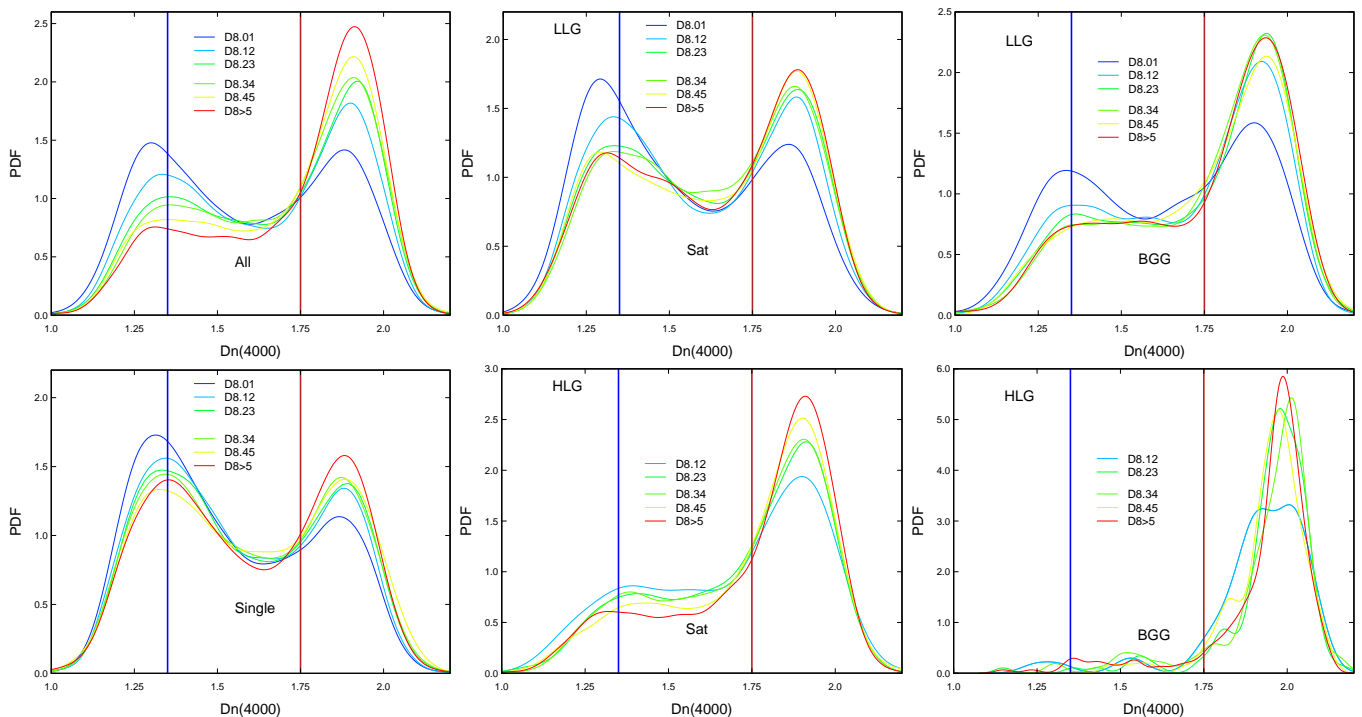


Fig. 9. Distribution of $D_n(4000)$ index of galaxies in various global density $D8$ regions. Upper left panel: all galaxies, upper middle panel: LLG (low-luminosity groups) satellite galaxies, upper right panel - LLG BGGs. Lower left panel: single galaxies, lower middle panel: HLG (high-luminosity groups) satellite galaxies, and lower right panel: HLG BGGs. Vertical lines show the values of $D_n(4000)$ index $D_n(4000) = 1.35$, and $D_n(4000) = 1.75$.

Table 2. Median values of the galaxy properties for single galaxies, and galaxies in LLGs and HLGs

(1)	(2)	(3)	(4)	(5)	(6)	(7)	(8)	(9)	(10)	(11)	(12)	(13)
ID	N_{gal}	F_{VO}	M_{med}^*		σ_{med}^*		C_{med}		$D_n(4000)_{med}$		SFR_{med}	
			VO	YS	VO	YS	VO	YS	VO	YS	VO	YS
<i>Single</i>	35530	0.31	10.71	10.40	160	89	0.34	0.42	1.89	1.40	-1.28	0.19
<i>Sat_{LLG}</i>	19106	0.39	10.63	10.38	155	88	0.35	0.42	1.89	1.41	-1.35	0.13
<i>BGG_{LLG}</i>	12133	0.54	10.97	10.66	192	108	0.33	0.41	1.92	1.46	-1.17	0.34
<i>Sat_{HLG}</i>	12062	0.61	10.72	10.47	167	96	0.35	0.41	1.91	1.49	-1.33	0.02
<i>BGG_{HLG}</i>	732	0.92	11.35	11.12	251	149	0.31	0.40	1.98	1.53	-1.00	0.34

Notes. Columns are as follows: (1): Population ID; (2): Number of galaxies in a population; (3): Percentage of VO galaxies in a population; (4–5): Median values of the stellar mass M_{med}^* for VO and YS galaxies; (6–7): Median values of the stellar velocity dispersion σ^* for VO and YS galaxies; (8–9): Median values of the concentration index C for VO and YS galaxies; (10–11): Median values of the $D_n(4000)$ index $D_n(4000)_{med}$ for VO and YS galaxies. (12–13): Median values of SFR index SFR_{med} for VO and YS galaxies.

the influence of other galaxies, the percentage of VO galaxies in superclusters is higher than in lower global density regions (36% versus 27%).

The percentage of VO galaxies among galaxies in HLGs is higher, spanning from 53% to 62% among satellite galaxies in the lowest and highest global density regions, and being larger than 92% among BGGs. We note that YS BGGs in HLGs lie in the lowest luminosity end of this group population, and only two of them have $D8 > 5$ at their location. In total, eight galaxies among BGGs of HLGs have $D_n(4000) < 1.35$.

In general, these trends reflect the well-known large-scale morphology–density relation (Einasto & Einasto 1987). However, there is an important difference. Typically, densities around galaxies have been calculated using the distance to Nth nearest neighbour, as in Einasto & Einasto (1987) and Bluck et al. (2020b). In the present study, we distinguish between group membership and global densities using the luminosity–density

field. This enables us to show that in groups of all luminosities and for single galaxies, galaxy populations in various global density regions are different.

3.3. The morphological properties of VO and YS galaxies in various global density environments

In our further analysis, we compare distributions of the stellar masses M^* , stellar velocity dispersions σ^* , concentration index C , and SFR of galaxies in various global density $D8$ intervals. Although galaxies were selected according to their $D_n(4000)$ index, we also compare the distributions of this index. We further divide galaxies into single, satellite galaxies in groups, or BGGs.

We begin this analysis with *VO galaxies*, and compare the stellar masses, M^* , stellar velocity dispersion, σ^* , and concentration index C of VO galaxies in various global density $D8$ regions. We applied the Kolmogorov-Smirnov (KS) test to esti-

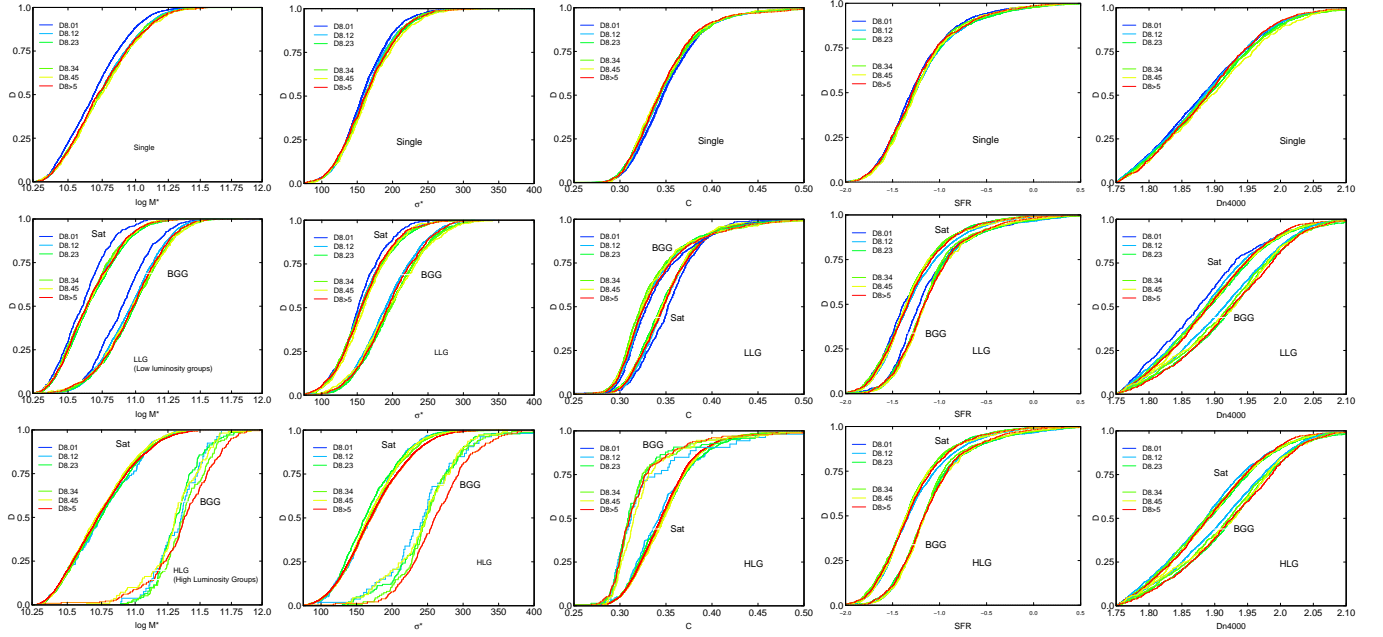


Fig. 10. VO galaxies: distributions of stellar mass M^* (leftmost panels), stellar velocity dispersion σ^* (second panels), concentration index C (third panels), log SFR (fourth panels), and $D_n(4000)$ index (rightmost panels) for single galaxies (upper row), satellite galaxies and BGGs of LLGs (thin lines; middle row), and satellite galaxies and BGGs of HLGs (thick lines; lower row) in various global density $D8$ intervals, as shows in the legends.

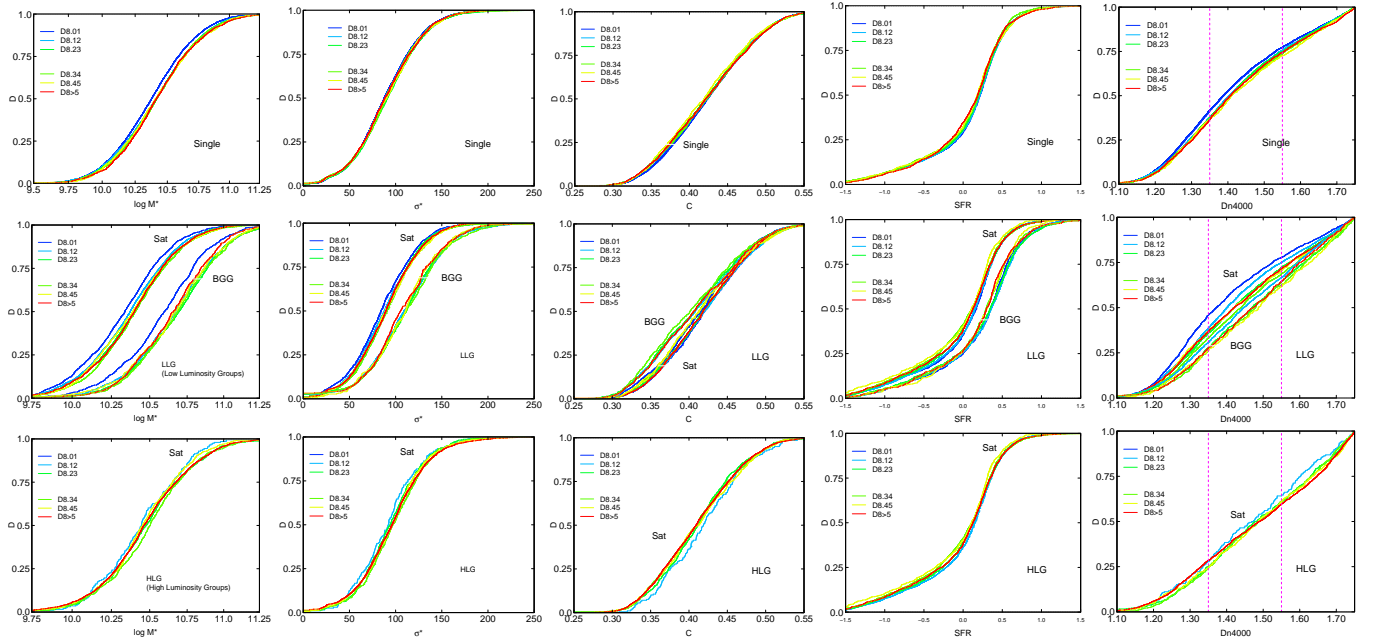


Fig. 11. YS galaxies: distributions of stellar mass M^* (leftmost panels), stellar velocity dispersion σ^* (second panels), concentration index C (third panels), log SFR (fourth panels), and $D_n(4000)$ index (rightmost panels) for single galaxies (upper row), satellite galaxies and BGGs of LLGs (thin lines; middle row), and satellite galaxies and BGGs of HLGs (thick lines; lower row) in various global density $D8$ intervals, as shows in the legends. In the rightmost panels, vertical lines indicate $D_n(4000)$ index values $D_n(4000) = 1.35$ and $D_n(4000) = 1.55$ (this value separates star forming and (recently) quenched galaxies).

mate the statistical significance of the differences between the galaxy populations. We consider that the differences between distributions are significant and highly significant when the p -value (the estimated probability of rejecting the hypothesis that the distributions are statistically similar) $p \leq 0.05$ and $p \leq 0.01$, respectively.

In Fig. 10 we show the distribution of stellar masses of galaxies with $D_n(4000) \geq 1.75$ in various global density $D8$ regions.

This figure shows that the largest difference is between the stellar masses of galaxies in the lowest global density region, $D8 < 1$, and all other global density regions $D8 > 1$. This difference is seen for all populations (single galaxies, satellite galaxies, and BGGs). This difference leads to a quantitative definition of the watershed region, that is, a region with global luminosity-density $D8 \leq 1$. The KS test results in Tables A.2 - A.1 show that the differences in stellar mass between the galaxies in the lowest

density regions and in all other global density regions are highly significant. Also, one can see that the stellar masses of satellite galaxies are the lowest, BGGs have the highest stellar masses, and the stellar masses of single galaxies have values between those of satellites and BGGs. We note that, on average, more than half of single and satellite galaxies, and more than 80 % of BGGs of LLGs, have stellar masses higher than the stellar mass of the Milky Way galaxy as given in Licquia & Newman (2015). All BGGs of HLGs have higher stellar masses than the Milky Way.

We used the KS test to compare stellar masses of galaxies in other global density regions ($1 < D8 < 2$ and so on). This comparison showed that, as also suggested by Fig. 10, stellar masses of galaxies from the same population (single galaxies, LLG satellite galaxies or BGGs, and HLG satellites or BGGs) are statistically similar with very high significance ($p > 0.05$, typically $p > 0.5$) with a few exceptions. BGGs of HLGs have higher stellar masses in global high-density environments. This is expected, as these groups are richer and of higher luminosity than HLGs in lower global density environments (Fig. 2, right panel). This comparison shows that although in the global density interval $1 < D8 < 2$ most galaxies are single or members of poor groups, as is also the case in the watershed region, these galaxies have already higher stellar masses and other properties similar to those of galaxies in higher global density regions where LLGs and HLGs dominate.

Similar, albeit weaker, trends are seen in the distribution of the stellar velocity dispersion of galaxies σ^* , in the distribution of the concentration index C , and in the distribution of SFR. We note that approximately 85%–90% of VO galaxies have $C < 0.38$, suggesting that these are mostly early-type galaxies. This is expected, and was shown in Einasto et al. (2020) using the probability of being an early-type galaxy. KS tests show that the differences in stellar velocity dispersion and the concentration index of galaxies in the lowest global density regions and elsewhere are statistically highly significant, and typically not significant between galaxies in other global density regions. There is a weak trend that BGGs in HLGs in low global density regions have lower stellar velocity dispersions than in the highest global density region. These are the same galaxies that have higher stellar masses than BGGs of HLGs in the lower global density regions.

We also looked at the distributions of the $D_n(4000)$ index of VO galaxies (Fig. 10). For single galaxies, the distribution of the $D_n(4000)$ index is the same in all global density environments. However, the $D_n(4000)$ index of galaxies in groups and especially for the brightest galaxies of groups (Fig. 10) shows that this index is the lowest in the lowest global density environment ($D8 < 1$). For satellites in HLGs, the trends with global environment are weaker. The BGGs have the lowest $D_n(4000)$ index values in the lowest global density environment, and the highest values of $D_n(4000)$ index in the highest global density environment. This suggests that they have older stellar populations. However, the differences in the distribution of the $D_n(4000)$ index between satellites and BGGs are much larger than the differences in $D_n(4000)$ between the same galaxy type in different global environments.

The average differences in the $D_n(4000)$ index values between the satellite VO galaxies in the lowest global density environment and in higher global density environments shown above may lead to the differences in the ages of stellar populations of up to approximately 2 Gyr (Kauffmann et al. 2003). In addition, BGGs of LLGs in the lowest global density environment have stopped their star formation later than the BGGs in high-

global-density environment. For HLGs, the trends with global density may also be affected by the increase in group richness with global density. For single galaxies, there is no clear trend in the age of stellar populations with global density environment.

Next we present a similar analysis for YS galaxies with $D_n(4000) < 1.75$ (Fig. 11 and Tables A.5 - A.4). Einasto et al. (2020) and Einasto et al. (2021b) divided galaxies with $D_n(4000) < 1.75$ into several subclasses: blue star forming galaxies with $D_n(4000) < 1.55$, and recently quenched and red star forming galaxies with $1.35 < D_n(4000) < 1.75$ (see Fig. 3 in Einasto et al. 2021b). Overall, from Fig. 11 it appears that the trends of galaxy properties with global density for YS galaxies are weaker than those for VO galaxies, although the KS test shows that YS galaxies have lower stellar masses in the lowest global density environments with very high statistical significance. Most YS galaxies have lower stellar masses than our Milky Way galaxy.

The distributions of the $D_n(4000)$ index for YS satellite galaxies, BGGs, and single galaxies in Fig. 11 show that these galaxies have lower $D_n(4000)$ index values in the lowest global density environment. YS LLG satellite galaxies have slightly lower stellar masses and lower $D_n(4000)$ index values in $1 < D8 < 2$ global density regions than in higher global density regions. These differences are highly significant.

On average, the median values of the $D_n(4000)$ index for galaxies in LLGs (both for satellites and BGGs) and for single galaxies in all environments are $D_n(4000) \approx 1.40$ (for BGGs, $D_n(4000) \approx 1.45$) which according to Kauffmann et al. (2003) corresponds to an age of the stellar populations of ≈ 0.95 Gyr. The stellar age differences between satellites and BGGs are small. Satellite galaxies in HLGs have slightly higher values of $D_n(4000)$ index, suggesting somewhat higher ages of their stellar populations. Among satellites of HLGs, there are more galaxies with $D_n(4000) > 1.35$, and therefore more galaxies that are already quenched or are now in transition (red, star forming, and recently quenched galaxies). These galaxies can be found preferentially in the infall zones of groups and clusters (Einasto et al. 2020, 2021b). This may be an indication that HLGs are dynamically more active than LLGs. The fraction of blue star forming galaxies with $D_n(4000) > 1.35$ is the highest among satellite galaxies of LLGs in the lowest global density environment, namely approximately 45%, where even $\approx 35\%$ of BGGs have $D_n(4000) > 1.35$. Approximately 30%–35% of BGGs and single galaxies have $D_n(4000) > 1.55$ which suggest that they may already be quenched.

The distribution of stellar velocity dispersion of YS galaxies σ^* shows that, on average, σ^* values are lower than those for VO galaxies, as expected in the case of star-forming galaxies. The concentration index C values for YS galaxies are higher than those of VO galaxies, and the percentage of late-type galaxies with $C > 0.38$ is larger than 25 % among them.

The trends that we see between global density and stellar velocity dispersion, concentration index, and SFRs of YS galaxies are very weak. This tells us that star-forming galaxies with young stellar populations are very similar in all environments from the lowest density watersheds to superclusters. This is confirmed by the results of the KS test.

We note that the relatively high percentage of YS galaxies among BGGs of LLGs should be taken with caution. We analysed the galaxy content of groups with between 5 and 9 member galaxies as such groups are more reliable than very poor groups. We found that typically, even if the most luminous galaxy in such a group is star forming, among the group member galaxies there is at least one quenched galaxy. It is possible that the

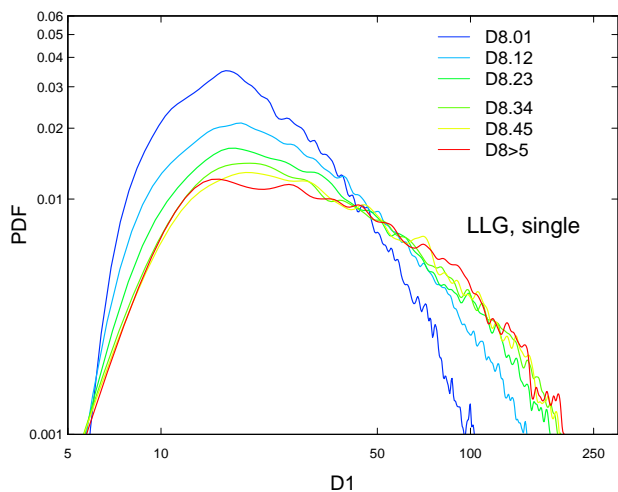


Fig. 12. Distributions of local luminosity densities $D1$ for single galaxies and for LLG galaxies in various intervals of global luminosity-density $D8$.

brightest galaxy in this case is not the central galaxy, and groups are still forming, as was concluded for richer groups and clusters in Einasto et al. (2012b). Furthermore, we only found three groups in the lowest global density environment, and four groups in the highest global density environment, in which all the galaxies have young stellar populations with $D_n(4000) < 1.35$. Three such groups are filament members (two in high-density environment, and one in low-density environment).

In summary, Figs. 10 and 11 present the distributions of morphological properties of galaxies for different global density $D8$ ranges in terms of group membership: single galaxies, satellite galaxies, and BGGs of LLGs and of HLGs. These figures demonstrate the similarity between galaxy properties over a wide range of group luminosities (and therefore masses). In particular, a remarkable similarity is observed between the distributions of morphological properties of single galaxies and satellites of HLGs. Figures 10 and 11 also show another important aspect of morphological properties of galaxies: great differences are seen between the distributions of morphological properties of satellites and BGGs, both in LLGs and HLGs. These figures show that group membership type is the major parameter determining the morphological properties of galaxies.

3.4. Local environments of single galaxies and groups with VO and YS BGGs

Table 1 shows that 27%–36% of single galaxies and 42%–59% of BGGs of LLGs are VO galaxies. The percentage of VO galaxies among these types of galaxies increases with global luminosity density. Next, we compare local environmental densities at the location of single galaxies and galaxies in LLGs, as well as at the location of VO and YS single galaxies and BGGs of LLGs.

Local luminosity-density around galaxies $D1$ is defined as the luminosity-density around galaxies calculated with a smoothing length of $1 h^{-1}$ Mpc. The distribution of local luminosity-densities $D1$ at the location of single galaxies and members of LLGs in various global luminosity-density $D8$ intervals is presented in Fig. 12. We do not show local densities around HLG member galaxies as these are absent in the lowest global density regions. Interestingly, these distributions show that in the global density interval $1 < D8 < 2$ local luminosity-densities $D1$ are higher than in watershed regions, but lower

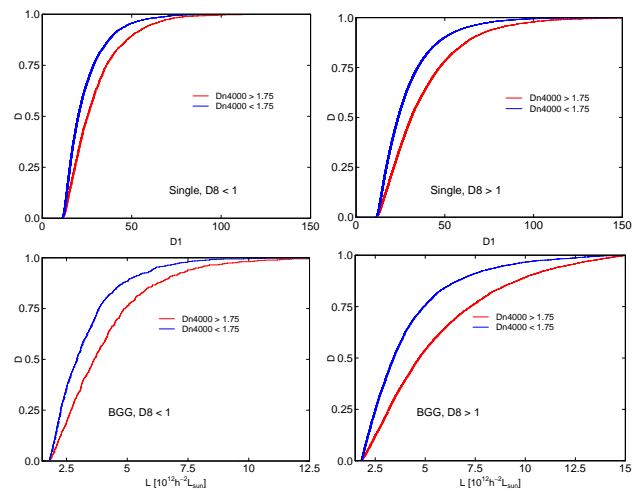


Fig. 13. Distributions of local luminosity densities $D1$ for single galaxies (upper row) and group luminosities L_{gr} for BGGs of LLGs (lower row) in global low-luminosity regions ($D8 \leq 1$, left panels) and global high-luminosity regions ($D8 > 1$, right panels). Red lines: Single galaxies and BGGs with $D_n(4000) > 1.75$ (VO galaxies). Blue lines: $D_n(4000) < 1.75$ (YS galaxies).

than in higher global density regions, where local densities at the location of single galaxies and LLGs are similar on average. Above, we show that the morphological properties of galaxies in global density regions $D8 > 1$ are already similar. We may be seeing evidence of an interplay between local and global densities in shaping group formation and the morphological properties of galaxies.

In Fig. 13, we present local environmental densities at the location of VO and YS single galaxies and BGGs of LLGs. In this figure, for BGGs we use group luminosities L_{gr} as a proxy for their local environment, and for single galaxies we apply the values of the luminosity-density field with smoothing length $1 h^{-1}$ Mpc, $D1$. Distributions of L_{gr} and $D1$ values separately for global luminosity densities $D8 \leq 1$ and $D8 > 1$ are given in Fig. 13.

Figure 13 shows that in all global environments, in the case of both single galaxies and BGGs, VO galaxies are located in higher local density environments than YS galaxies. Among single galaxies, in watershed regions ($D8 \leq 1$) VO galaxies have median values $D1_{med} = 25$, while galaxies with young stellar populations have $D1_{med} = 20$. In regions of higher global density, ($D8 > 1$) single VO galaxies have median values $D1_{med} = 31$, and YS galaxies have $D1_{med} = 24$.

VO BGGs in watershed regions lie in groups with median luminosity with $L_{gr}^{med} = 3.6 \times 10^{10} h^{-2} L_{\odot}$, while YS BGGs have $L_{gr}^{med} = 2.9 \times 10^{10} h^{-2} L_{\odot}$. In higher global density regions, the median value of host group luminosity for VO BGGs $L_{gr}^{med} = 4.7 \times 10^{10} h^{-2} L_{\odot}$ and for YS BGGs $L_{gr}^{med} = 3.4 \times 10^{10} h^{-2} L_{\odot}$. The KS test shows that the differences between local densities (group luminosities for BGGs) are statistically very highly significant, with KS test p value $p < 0.001$. Therefore, in global high-density environments, higher local densities lead to a higher percentage of quenched galaxies even in groups of the same luminosity.

4. Analysis of the results and discussion

4.1. Does global density matter?

In this study, our aim is to find out whether global density, quantified with the luminosity–density field, has any influence on the galaxy content of the cosmic web. Our results reveal that the global density most strongly affects the group content of a given environment. The lowest global density environments (watersheds between superclusters with $D8 < 1$) are populated by single galaxies, which form more than 70 % of galaxy populations there, and by galaxies in poor, low-luminosity groups. In contrast, the highest global density environments (superclusters) are mostly populated by high-luminosity groups and clusters, although even in these environments single galaxies form approximately one-sixth of all galaxies. This means that global and local environmental densities are correlated: local densities are higher, on average, at higher global densities.

The effect of global density on the star formation properties of galaxies is less strong. Surprisingly, still almost one-third of all galaxies in the lowest global density environments with $D8 \leq 1$ have $D_n(4000)$ index values $D_n(4000) > 1.75$. In the highest global density environments, more than half of all galaxies have such high values of $D_n(4000)$ index. Even among single galaxies and satellites of LLGs (for which the local densities are the lowest), the percentage of galaxies with $D_n(4000) > 1.75$ is 27 – 30. These galaxies can be considered as quenched, with old stellar populations. Only approximately 2% of galaxies with $D_n(4000) > 1.75$ may still form stars, and their high $D_n(4000)$ index values may be related to their metallicity. Therefore, the percentage of VO galaxies at the lowest densities is relatively high. The percentage of galaxies with $D_n(4000) > 2$ increases from approximately 2 % in watershed regions to 7 % in superclusters. Up to almost 40 % of BGGs of HLGs have such high $D_n(4000)$ indexes, which indicates that they have not changed significantly over the last 10 Gyr, since redshifts of $z \approx 1.5 - 2$.

Also somewhat surprisingly, we found that the effect of global density is the weakest on other galaxy properties, such as their stellar masses, concentration indexes, and stellar velocity dispersions. These parameters are almost the same in all global density environments, except in the regions of lowest density. In watershed regions with threshold density $D8 = 1$, stellar masses and stellar velocity dispersions of galaxies from all types of systems (single galaxies, satellites, and BGGs) are lower than in higher global density environments, and their concentration index is higher. We point out that all this holds for single galaxies, satellites, and BGGs, and is therefore independent of local density. This small but statistically significant difference may be an indicator that, at some level, global density is also important in this case. Evidence in support of this hypothesis is provided by the finding that although in the global density interval $1 < D8 < 2$ most galaxies are still singles or members of LLGs, as also in the watershed region, these galaxies have morphological properties similar to those of galaxies in higher global density regions where LLGs and HLGs dominate.

In all global density environments, the properties of single galaxies are between those of satellite galaxies in LLGs and HLGs. Interestingly, satellite galaxies in HLGs are close in their properties to the BGGs of LLGs. BGGs of HLGs are different from BGGs in LLGs, especially in the highest global density environments (superclusters). There are almost no star-forming galaxies among the BGGs of HLGs, and they have higher stellar masses and stellar velocity dispersions, and lower concentration indexes than their counterparts in LLGs. Next, we discuss what these results tell us about the evolution of galaxies and groups.

4.2. Coevolution of galaxies and groups in the cosmic web

Star formation quenching in single galaxies and LLG members: cosmic web detachment. In the lowest global density (watershed) regions, single VO galaxies and VO members of LLGs are somewhat different from those in other global density regions: their median stellar mass is lower, and among them there is a lower percentage of galaxies with extremely old stellar populations. This can be referred to as ‘environmental downsizing’. These are still quenched VO galaxies, but their growth is not like that seen in denser environments. As we show, even in the global density interval $1 < D8 < 2$, where single galaxies and members of LLG still dominate, the morphological properties of VO galaxies are similar to those in higher global density environments.

Due to very low environment density and lower stellar mass, one may conclude that for these galaxies, mergers were suppressed but the galaxies are still quenched. Therefore, we might wonder what caused star formation quenching in these environments. The answer may be cessation of fresh gas supply due to the detachment of primordial filaments as a galaxy enters a group (cosmic web detachment (CWD)), which was theoretically predicted from simulations by Aragon Calvo et al. (2019) (see also Lacerna et al. 2016). Also, gas may be removed in galaxies due to ram pressure as they fly across filaments of the cosmic web. However, the efficiency of this process is not yet clear. In addition, in the case of single VO galaxies the problem remains that for these processes there needs to be a significant amount of presently undetected LLGs or filaments.

Local densities at the locations of VO galaxies are higher than at the locations of YS galaxies. This may be related to the distribution of filaments in various global environments. Similar trends within filaments were noted by Lee et al. (2021). From observations, we do not have information on primordial filaments, but present-day galaxy filaments are closer together in superclusters than in the low-density environment around them (Einasto et al. 2020). Therefore, the probability that a galaxy will encounter a filament is higher in high-global-density environments, and this makes CWD more effective in high-density environments. This in turn leads to a higher percentage of VO galaxies in the high-global-density environments, even among single galaxies in superclusters in comparison with watershed regions.

Preprocessing of galaxies: single galaxies and satellites versus BGGs, and LLGs versus HLGs. The lowest stellar masses of galaxies in this study are $M^* = 1.8 \times 10^{10} M_\odot$. Due to this cut-off, we may not know all possible galaxy filaments. Detachment of the primordial filaments of VO galaxies in cosmic watersheds may be due to interactions with these undetected present-day filaments. But this is not the only reason.

The high fraction of VO galaxies among single galaxies and in poor groups is clear evidence of the preprocessing of galaxies before falling into clusters, as shown for high-redshift clusters by Werner et al. (2021), who found that at $z \sim 1$ most massive galaxies were self-quenched or preprocessed in groups before falling into clusters. Isolated elliptical galaxies have also been found in filaments around Coma cluster in the Coma supercluster (Lacerna et al. 2016). In the AMIGA sample of isolated galaxies, elliptical and lenticular galaxies make up 14 % (Sulentic et al. 2006). Among the galaxies analysed in the present study, approximately 50% of those in LLGs and approximately 40% of the galaxies in HLGs and single galaxies are members of filaments. We find that approximately 25% of filament member galaxies from all populations (single galaxies, LLG members,

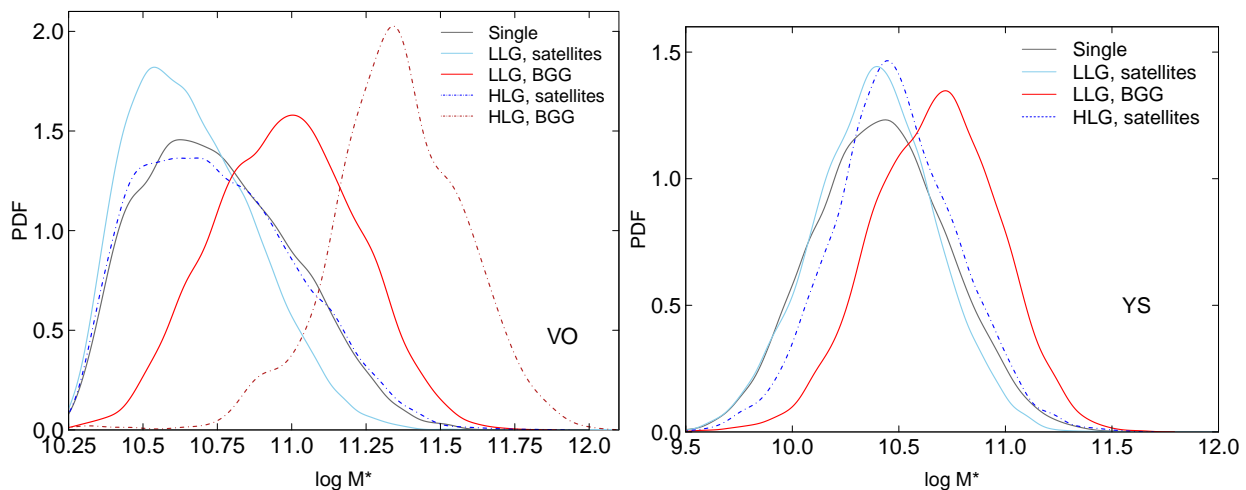


Fig. 14. Distributions of stellar mass M^* for single galaxies (grey lines), satellites galaxies in LLGs and HLGs (light and dark blue lines, respectively), and BGGs of LLGs and HLGs (light red and dark red lines, respectively) for VO galaxies (left panel) and YS galaxies (right panel) in global luminosity–density regions $D8 > 1$. Solid lines show single galaxies and LLG members, and dot-dashed lines show HLG members.

and HLG members) have $D_n(4000) \geq 1.75$. Therefore, pre-processing occurs also in filaments (Einasto 1992; Tempel et al. 2014a; Kraljic et al. 2018; Kuutma et al. 2020; Castignani et al. 2022b; Edwards et al. 2021; Castignani et al. 2022a; Jhee et al. 2022). A dedicated and detailed analysis of galaxy quenching in filaments in various global density environments is merited.

Next, we discuss other mechanisms in addition to the CWD that affect galaxy properties and may lead to star-formation quenching in galaxies. Various data point to accretion events and a wide range of merger scenarios in the history of the MW-like galaxies 11 – 8 Gyr ago (Haywood et al. 2016; Bell et al. 2017; Di Matteo et al. 2019; Quilley & de Lapparent 2022). Accretion and merger events at least 4 Gyr ago may also have occurred in isolated elliptical galaxies (Lacerna et al. 2016; Mazzei et al. 2022), and these could disturb gas inflow from primordial filaments. This variety is interesting in the context of our study, which reveals similarities in the morphological properties of single galaxies and satellites of LLGs in very different global environments. Also, could the very different percentages of VO galaxies among single galaxies in low- and high-global-density environment be related to the variety of accretion histories of galaxies, with quenching being more effective in high-global-density environment?

The efficiency of the star-formation quenching of satellite galaxies as they fall into a potential well of a main galaxy (in the case of single galaxies) or of a group (for satellite galaxies in groups) depends on their orbital parameters (Łokas 2020; Rodríguez et al. 2022). Typically, it takes more than one peripassage to quench a satellite galaxy. The star formation in galaxies decreases under environmental processes described as slow-then-rapid quenching with characteristic timescales of 4 – 5 Gyr (Muzzin et al. 2014; McGee et al. 2014; Maier et al. 2019; Kipper et al. 2021; Kuschel et al. 2022). Slow quenching by strangulation and overconsumption starts when a galaxy enters a group and gas inflow stops. When a galaxy reaches the central parts of a group or cluster, star formation is stopped by ram pressure which strips gas from galaxies. These timescales agree well with our finding that galaxies in the central parts of groups have $D_n(4000) > 1.75$, that is, they were quenched several gigayears ago. As the galaxies orbit the group or cluster with many pericenter passages, their shapes change from disky to triaxial, and their rotation is suppressed and replaced by random

motions while they become increasingly red (Łokas 2020). This may take at least 4 Gyr from the first pericenter passage (Łokas 2020), which agrees with our findings about the ages of stellar populations of VO galaxies in groups and clusters. This may lead to the differences in concentration index that we find for the galaxies included in our study. Only rarely is the impact directed towards the BGG in a group, which could lead to the merger of both galaxies and changes in the morphological properties of the BGGs.

To better understand the influence of group membership on the distributions of morphological properties of galaxies, we show in Fig. 14 the distribution of stellar masses M^* for galaxies in global density regions $D8 > 1$ in different group membership classes, separately for VO and YS galaxies. Watershed galaxies with clearly lower stellar masses than galaxies from the same class in other global luminosity–density regions are not taken into account in this figure. Figure 14 shows that the stellar mass M^* distributions of satellites of LLGs and HLGs are very similar. The M^* distributions for single galaxies are also close, but for VO galaxies they are slightly shifted towards smaller stellar masses. These similarities suggest that some HLG satellites may have been single galaxies in the past. For example, McGee et al. (2009) found that approximately 40% of galaxies falling into groups and clusters are single galaxies and not members of groups. This interpretation agrees with the changes of the percentage of single galaxies and galaxies in LLGs and HLGs seen in Fig. 7. While the percentage of galaxies in LLGs remains almost unchanged over a wide range of global luminosity densities, the percentage of single galaxies decreases and the percentage of galaxies in HLGs increases. The enhanced fraction of star-forming galaxies among single galaxies in comparison with HLG satellites (Figs. 5 and 9) can be explained as evidence of star-formation triggering in galaxies while they fall into groups and clusters. The slight differences in distributions for single galaxies and satellites of LLGs can be interpreted as evidence that the sample of satellite galaxies of LLGs contains some galaxies that are statistically less massive than our sample of single galaxies. The distinction between satellites and single galaxies also depends on the parameters used to compile group catalogues and the magnitude limits of galaxies in the sample. The connection between satellites and single galaxies is an interesting question by itself, and deserves a dedicated study.

Also, considering low local densities $D1$ at the location of LLGs, even in global high-density environments shown in Fig. 12, it is possible that LLGs form at locations where the local density is sufficient for the formation of a poor group, but not yet sufficient for the formation of a rich group or cluster.

The distributions for BGGs are shifted in respect to satellites towards larger masses by a factor of about three, and the shapes of the distributions are also different. These differences suggest that, in terms of mass, the growth of BGGs is governed by processes that are essentially different from those governing the growth of all other galaxies.

The $D_n(4000)$ index values of VO galaxies in $D8 < 1$ regions suggest that their stellar populations may be up to 2 Gyr younger than in VO galaxies from higher global density environments. The percentage of galaxies with $D_n(4000) \geq 2.0$ among single galaxies is about 5%–10%. In all global environments, approximately 10 % of poor group satellite galaxies and 20 % of their BGGs have $D_n(4000) \geq 2.0$. Among rich groups, about 15%–20% of satellite galaxies and about 40 % of the BGGs have $D_n(4000) \geq 2.0$. These galaxies form a high-end tail in the stellar mass and σ^* distributions. According to Kauffmann et al. (2003), such high values of the $D_n(4000)$ index correspond to ages of the stellar population in these galaxies of at least 10 Gyr, that is, these galaxies stopped forming stars at redshifts $z \approx 1.5 - 2$ (see also Bezanson et al. 2012; Chu et al. 2021). This is approximately the redshift of the morphology–density relation reversal: at higher redshifts, high-density regions are populated by star-forming galaxies that quenched faster than similar galaxies in lower density environments, causing the reversal of the relation at lower redshifts at which high-density regions are populated by quenched galaxies (Chiang et al. 2017; Hwang et al. 2019, and references therein). Even so, observations have found quenched galaxies in protoclusters even at redshifts as high as $z = 3.37$ (McConachie et al. 2022).

Lin et al. (2019) used the MaNGA data to study the quenching of galaxies in different local environments at submegaparsec scale, which is defined by halo mass, that is, luminosity-based group mass in which a galaxy resides. These authors showed that the dominant mechanism is inside-out quenching where quenching first takes place in the central region and then proceeds outwards. This effect is dominant for central galaxies and high-mass satellites, but is weaker for low-mass satellites with stellar masses $\log M^* < 10.5$ (see also Kipper et al. 2021). This agrees well with our results, which showed that the percentage of galaxies with $\log M^* < 10.5$ is lower than 20 % among satellite galaxies with $D_n(4000) > 1.75$, and there are almost no BGGs with such low stellar mass. Almost half of YS galaxies with $D_n(4000) < 1.75$ (25 % of BGGs) have stellar masses $\log M^* < 10.5$ (Figs. 10 and 11).

The connection between the evolution of groups and the galaxies within them is also seen in the star-formation properties of the BGGs: while BGGs in low-luminosity groups may still be star-forming, in high-luminosity groups almost all BGGs are quenched. Even in low-luminosity groups with star-forming BGGs, typically at least one galaxy is quenched and may become a BGG during subsequent evolution of galaxies and the whole group. We found very few groups (among groups with $5 < N_{gal} < 10$) for which all the galaxies within have $D_n(4000) < 1.35$. The star-formation properties of BGGs and single galaxies also depend on the local environment: those in a lower local density environment are more likely to be actively star-forming. Differences in the morphological properties of the BGGs and satellites suggest that BGGs have been through a special as-

sembly history with a series of mergers during their evolution (Liu et al. 2015; Edwards et al. 2020).

The similarity in the properties of galaxies found in different environments revealed by the present study has been detected before. In a review paper about galaxy properties Blanton & Moustakas (2009) noted that when galaxy mass and star formation history are fixed, other properties of galaxies are the same over a range of different environments, with these different environments being typically defined using the N th nearest neighbour of a galaxy, or their membership to clusters or groups. Balogh & McGee (2010) found that the properties of galaxies in groups from a wide range of masses on a two-colour diagram are very homogeneous. Questions as to why there are different types of galaxies (elliptical and spirals), and why their properties are almost independent of environment were recently discussed in Peebles (2021) and Peebles (2022), in which a series of unanswered questions about galaxy formation and evolution were outlined.

Here we outlined how the evolution of galaxies and groups leads to the higher fraction of quenched galaxies in high-density environments, known as the large-scale morphology-density relation. In our study, we used global luminosity density field to study galaxy environments, and divided galaxies according to their group membership. Our analysis shows that once we fix whether a galaxy is single, a satellite galaxy in a group, or a BGG, galaxy properties are almost independent of the global environment. We propose various processes that could lead to very similar galaxies in hugely varying environments where conditions are very different.

5. Summary

Here we present a study of group content and galaxy population in various global density environments. We summarise our results as follows:

- 1) Based on galaxy and group properties, we define the watershed regions as regions with global luminosity–density $D8 \leq 1$. Watersheds occupy approximately 65% of the total SDSS volume.
- 2) The strongest effects of global environment are seen in the richness of groups. Watershed regions are mostly populated by single galaxies (70% of all galaxies) and poor, low-luminosity galaxy groups with $L_{gr} \leq 15 \times 10^{10} h^{-2} L_{\odot}$. Richer and more luminous groups and clusters reside in higher global density regions.
- 3) Global environment affects the star-formation properties of galaxies less strongly. In the watershed regions, approximately 30% of all galaxies (including single galaxies) have very old stellar populations with $D_n(4000) > 1.75$ (VO galaxies). In the highest global density environments (super-clusters), VO galaxies form 55% of all galaxies.
- 4) The weakest effects of global environment are seen in the morphological properties of galaxies. Single galaxies and satellites in watersheds have lower stellar masses and lower stellar velocity distributions than their counterparts in higher global environments. In higher global density environments with $D8 > 1$, the stellar masses, stellar velocity dispersions and concentration indexes of galaxies from a given class (i.e. single galaxies, satellites, and BGGs), or, in other words, over a wide range of group luminosities (and therefore masses), are statistically similar.
- 5) Morphological properties of galaxies are mainly determined by whether a galaxy is a single, satellite, or BGG. The largest

differences in galaxy properties in all environments are between BGGs and all other galaxies (satellites of groups and single galaxies). BGGs have higher stellar masses, larger stellar velocity dispersions, and lower concentration indexes than other galaxies.

5.1) BGGs of poor groups may have old and young stellar populations, but BGGs of rich groups are almost all VOs.

5.2) Up to 40% of BGGs have $D_n(4000) > 2$, which suggests that these galaxies stopped star formation approximately 10 Gyr ago, at redshifts $z \approx 1.5 - 2$.

The similarity of galaxy properties in hugely varying environments where conditions are very different suggests that the present-day galaxy properties are largely shaped by their birthplace in the cosmic web (initial conditions for galaxy formation)—which determines whether a galaxy remains single or becomes a member of a poor group or a rich cluster—and internal processes that lead to star formation quenching in galaxies.

To better understand the formation and evolution of galaxies in various global and local environments, a next step is to analyse the morphological properties of galaxies in more detail than in the present study. For this purpose, one could use data on galaxies in our local cosmic neighbourhood, such as those provided by Quilley & de Lapparent (2022), and future multi-wavelength surveys with detailed information on galaxies, such as the J-PAS survey, or the HI Westerbork Coma Survey (Molnár et al. 2022), which showed that cluster galaxies are HI deficient in comparison with galaxies found around the cluster. Were galaxies born similar, turning into ellipticals or spirals during evolution in hugely different environments, or are the seeds of primeval galaxies already different? Of special interest for answering such questions is the star formation quenching in single galaxies in the lowest global density environments far from other galaxy systems where the influence of external factors to galaxy evolution is the smallest.

Acknowledgements. We thank the referee for detailed comments and suggestions which helped us to improve the paper. We thank Mirt Gramann for useful discussions. We are pleased to thank the SDSS Team for the publicly available data releases. Funding for the Sloan Digital Sky Survey (SDSS) and SDSS-II has been provided by the Alfred P. Sloan Foundation, the Participating Institutions, the National Science Foundation, the U.S. Department of Energy, the National Aeronautics and Space Administration, the Japanese Monbukagakusho, and the Max Planck Society, and the Higher Education Funding Council for England. The SDSS website is <http://www.sdss.org/>. The SDSS is managed by the Astrophysical Research Consortium (ARC) for the Participating Institutions. The Participating Institutions are the American Museum of Natural History, Astrophysical Institute Potsdam, University of Basel, University of Cambridge, Case Western Reserve University, The University of Chicago, Drexel University, Fermilab, the Institute for Advanced Study, the Japan Participation Group, The Johns Hopkins University, the Joint Institute for Nuclear Astrophysics, the Kavli Institute for Particle Astrophysics and Cosmology, the Korean Scientist Group, the Chinese Academy of Sciences (LAMOST), Los Alamos National Laboratory, the Max-Planck-Institute for Astronomy (MPIA), the Max-Planck-Institute for Astrophysics (MPA), New Mexico State University, Ohio State University, University of Pittsburgh, University of Portsmouth, Princeton University, the United States Naval Observatory, and the University of Washington. The present study was supported by the ETAG projects PRG1006, PSG700, and by the European Structural Funds grant for the Centre of Excellence "The Dark Side of the Universe" (TK133). This work has also been supported by ICRAnet through a professorship for Jaan Einasto. We applied in this study R statistical environment (Ihaka & Gentleman 1996).

References

Ahn, C. P., Alexandroff, R., Allende Prieto, C., et al. 2014, *ApJS*, 211, 17
 Aihara, H., Allende Prieto, C., An, D., et al. 2011, *ApJS*, 193, 29
 Alfaro, I. G., Rodriguez, F., Ruiz, A. N., Luparello, H. E., & Lambas, D. G. 2022, *A&A*, 665, A44

Aragon Calvo, M. A., Neyrinck, M. C., & Silk, J. 2019, *The Open Journal of Astrophysics*, 2, 7
 Bahcall, N. A., Gramann, M., & Cen, R. 1994, *ApJ*, 436, 23
 Balogh, M. L. & McGee, S. L. 2010, *MNRAS*, 402, L59
 Balogh, M. L., Morris, S. L., Yee, H. K. C., Carlberg, R. G., & Ellingson, E. 1999, *ApJ*, 527, 54
 Bell, E. F., Monachesi, A., Harmsen, B., et al. 2017, *ApJL*, 837, L8
 Bezanson, R., van Dokkum, P., & Franx, M. 2012, *ApJ*, 760, 62
 Blanton, M. R., Dalcanton, J., Eisenstein, D., et al. 2001, *AJ*, 121, 2358
 Blanton, M. R., Hogg, D. W., Bahcall, N. A., et al. 2003, *ApJ*, 592, 819
 Blanton, M. R. & Moustakas, J. 2009, *ARA&A*, 47, 159
 Blanton, M. R. & Roweis, S. 2007, *AJ*, 133, 734
 Bluck, A. F. L., Maiolino, R., Brownson, S., et al. 2022, *A&A*, 659, A160
 Bluck, A. F. L., Maiolino, R., Piotrowska, J. M., et al. 2020a, *MNRAS*, 499, 230
 Bluck, A. F. L., Maiolino, R., Sánchez, S. F., et al. 2020b, *MNRAS*, 492, 96
 Boselli, A. & Gavazzi, G. 2006, *PASP*, 118, 517
 Brinchmann, J., Charlot, S., White, S. D. M., et al. 2004, *MNRAS*, 351, 1151
 Brownson, S., Bluck, A. F. L., Maiolino, R., & Jones, G. C. 2022, *MNRAS*, 511, 1913
 Bruzual, G. & Charlot, S. 2003, *MNRAS*, 344, 1000
 Cappellari, M. & Emsellem, E. 2004, *PASP*, 116, 138
 Castignani, G., Combes, F., Jablonka, P., et al. 2022a, *A&A*, 657, A9
 Castignani, G., Vulcani, B., Finn, R. A., et al. 2022b, *ApJS*, 259, 43
 Chiang, Y.-K., Overzier, R. A., Gebhardt, K., & Henriques, B. 2017, *ApJL*, 844, L23
 Chu, A., Durret, F., & Márquez, I. 2021, *A&A*, 649, A42
 Contini, E., Gu, Q., Ge, X., et al. 2020, *ApJ*, 889, 156
 Croton, D. J., Springel, V., White, S. D. M., et al. 2006, *MNRAS*, 365, 11
 Davis, M. 1998, in *The Age of the Universe, Dark Matter, and Structure Formation*, 78–81
 Di Matteo, P., Haywood, M., Lehnert, M. D., et al. 2019, *A&A*, 632, A4
 Dressler, A. 1980, *ApJ*, 236, 351
 Driver, S. P., Bellstedt, S., Robotham, A. S. G., et al. 2022, *MNRAS*, 513, 439
 Džudžar, R., Kilborn, V., Murugesan, C., et al. 2019, *MNRAS*, 490, L6
 Edwards, L. O. V., Durret, F., Márquez, I., & Zhang, K. 2021, *AJ*, 161, 255
 Edwards, L. O. V., Salinas, M., Stanley, S., et al. 2020, *MNRAS*, 491, 2617
 Einasto, J., Jaaniste, J., Jõeveer, M., et al. 1974a, *Tartu Astrofüüsika Observaatorium Teated*, 48, 3
 Einasto, J., Jõeveer, M., & Saar, E. 1980, *MNRAS*, 193, 353
 Einasto, J., Klypin, A., Hütsi, G., Liivamägi, L. J., & Einasto, M. 2021a, *A&A*, 652, A94
 Einasto, J., Saar, E., Kaasik, A., & Chernin, A. D. 1974b, *Nature*, 252, 111
 Einasto, J., Suhhonenko, I., Hütsi, G., et al. 2011, *A&A*, 534, A128
 Einasto, J., Suhhonenko, I., Liivamägi, L. J., & Einasto, M. 2018a, *A&A*, 616, A141
 Einasto, J., Suhhonenko, I., Liivamägi, L. J., & Einasto, M. 2019, *A&A*, 623, A97
 Einasto, M. 1991, *MNRAS*, 252, 261
 Einasto, M. 1992, *MNRAS*, 258, 571
 Einasto, M., Deshev, B., Lietzen, H., et al. 2018b, *A&A*, 610, A82
 Einasto, M., Deshev, B., Tenjes, P., et al. 2020, *A&A*, 641, A172
 Einasto, M. & Einasto, J. 1987, *MNRAS*, 226, 543
 Einasto, M., Einasto, J., Müller, V., Heinämäki, P., & Tucker, D. L. 2003, *A&A*, 401, 851
 Einasto, M., Einasto, J., Tago, E., et al. 2007a, *A&A*, 464, 815
 Einasto, M., Kipper, R., Tenjes, P., et al. 2021b, *A&A*, 649, A51
 Einasto, M., Lietzen, H., Tempel, E., et al. 2014, *A&A*, 562, A87
 Einasto, M., Liivamägi, L. J., Tempel, E., et al. 2012a, *A&A*, 542, A36
 Einasto, M., Saar, E., Liivamägi, L. J., et al. 2007b, *A&A*, 476, 697
 Einasto, M., Suhhonenko, I., Heinämäki, P., Einasto, J., & Saar, E. 2005, *A&A*, 436, 17
 Einasto, M., Vennik, J., Nurmi, P., et al. 2012b, *A&A*, 540, A123
 Fujita, Y. 2004, *PASJ*, 56, 29
 Gómez, P. L., Nichol, R. C., Miller, C. J., et al. 2003, *ApJ*, 584, 210
 Goto, T., Yamauchi, C., Fujita, Y., et al. 2003, *MNRAS*, 346, 601
 Graham, A. W., Driver, S. P., Petrosian, V., et al. 2005, *AJ*, 130, 1535
 Gunn, J. E. & Gott, J. Richard, I. 1972, *ApJ*, 176, 1
 Haywood, M., Lehnert, M. D., Di Matteo, P., et al. 2016, *A&A*, 589, A66
 Henriques, B. M. B., White, S. D. M., Lilly, S. J., et al. 2019, *MNRAS*, 485, 3446
 Huchra, J. P. & Geller, M. J. 1982, *ApJ*, 257, 423
 Hwang, H. S., Shin, J., & Song, H. 2019, *MNRAS*, 489, 339
 Ihaka, R. & Gentleman, R. 1996, *Journal of Computational and Graphical Statistics*, 5, 299
 Jõeveer, M., Einasto, J., & Tago, E. 1978, *MNRAS*, 185, 357
 Jhee, H., Song, H., Smith, R., et al. 2022, arXiv e-prints, arXiv:2201.09540
 Kauffmann, G., Heckman, T. M., White, S. D. M., et al. 2003, *MNRAS*, 341, 33
 Kipper, R., Tamm, A., Tempel, E., de Propriis, R., & Ganeshiah Veena, P. 2021, *A&A*, 647, A32
 Komatsu, E., Smith, K. M., Dunkley, J., et al. 2011, *ApJS*, 192, 18

- Kraljic, K., Arnouts, S., Pichon, C., et al. 2018, *MNRAS*, 474, 547
- Kuschel, M., Scarlata, C., Mehta, V., et al. 2022, arXiv e-prints, arXiv:2205.12169
- Kuutma, T., Poudel, A., Einasto, M., et al. 2020, *A&A*, 639, A71
- Lacerna, I., Hernández-Toledo, H. M., Avila-Reese, V., Abonza-Sane, J., & del Olmo, A. 2016, *A&A*, 588, A79
- Lee, Y., Kim, S., Rey, S.-C., & Chung, J. 2021, *ApJ*, 906, 68
- Licquia, T. C. & Newman, J. A. 2015, *ApJ*, 806, 96
- Lietzen, H., Tempel, E., Heinämäki, P., et al. 2012, *A&A*, 545, A104
- Liivamägi, L. J., Tempel, E., & Saar, E. 2012, *A&A*, 539, A80
- Lin, L., Hsieh, B.-C., Pan, H.-A., et al. 2019, *ApJ*, 872, 50
- Liu, F. S., Lei, F. J., Meng, X. M., & Jiang, D. F. 2015, *MNRAS*, 447, 1491
- Łokas, E. L. 2020, *A&A*, 638, A133
- Maier, C., Ziegler, B. L., Haines, C. P., & Smith, G. P. 2019, *A&A*, 621, A131
- Matteucci, F., Panagia, N., Pipino, A., et al. 2006, *MNRAS*, 372, 265
- Mazzei, P., Rampazzo, R., Marino, A., et al. 2022, *ApJ*, 927, 124
- McConachie, I., Wilson, G., Forrest, B., et al. 2022, *ApJ*, 926, 37
- McGee, S. L., Balogh, M. L., Bower, R. G., Font, A. S., & McCarthy, I. G. 2009, *MNRAS*, 400, 937
- McGee, S. L., Bower, R. G., & Balogh, M. L. 2014, *MNRAS*, 442, L105
- Molnár, D. C., Serra, P., van der Hulst, T., et al. 2022, *A&A*, 659, A94
- Moore, B., Katz, N., Lake, G., Dressler, A., & Oemler, A. 1996, *Nature*, 379, 613
- Muldrew, S. I., Hatch, N. A., & Cooke, E. A. 2015, *MNRAS*, 452, 2528
- Muzzin, A., van der Burg, R. F. J., McGee, S. L., et al. 2014, *ApJ*, 796, 65
- Nulsen, P. E. J. 1982, *MNRAS*, 198, 1007
- Nusser, A., Dekel, A., Bertschinger, E., & Blumenthal, G. R. 1991, *ApJ*, 379, 6
- Park, C. & Choi, Y.-Y. 2009, *ApJ*, 691, 1828
- Park, C., Choi, Y.-Y., Vogeley, M. S., et al. 2007, *ApJ*, 658, 898
- Park, C., Lee, J., Kim, J., et al. 2022, *ApJ*, 937, 15
- Pasquali, A., Smith, R., Gallazzi, A., et al. 2019, *MNRAS*, 484, 1702
- Paulino-Afonso, A., Sobral, D., Darvish, B., et al. 2020, *A&A*, 633, A70
- Peebles, P. J. E. 2021, arXiv e-prints, arXiv:2106.02672
- Peebles, P. J. E. 2022, *MNRAS*, 511, 5093
- Postman, M. & Geller, M. J. 1984, *ApJ*, 281, 95
- Quilley, L. & de Lapparent, V. 2022, arXiv e-prints, arXiv:2206.04707
- Rodríguez, S., García Lambas, D., Padilla, N. D., et al. 2022, *MNRAS*, 514, 6157
- Ruiz-Lara, T., Few, C. G., Gibson, B. K., et al. 2016, *A&A*, 586, A112
- Salim, S., Rich, R. M., Charlot, S., et al. 2007, *ApJS*, 173, 267
- Sarzi, M., Falcón-Barroso, J., Davies, R. L., et al. 2006, *MNRAS*, 366, 1151
- Strateva, I., Ivezić, Ž., Knapp, G. R., et al. 2001, *AJ*, 122, 1861
- Suhhonenko, I., Einasto, J., Liivamägi, L. J., et al. 2011, *A&A*, 531, A149
- Sulentic, J. W., Verdes-Montenegro, L., Bergond, G., et al. 2006, *A&A*, 449, 937
- Tempel, E., Einasto, J., Einasto, M., Saar, E., & Tago, E. 2009, *A&A*, 495, 37
- Tempel, E., Saar, E., Liivamägi, L. J., et al. 2011, *A&A*, 529, A53
- Tempel, E., Stoica, R. S., Kipper, R., & Saar, E. 2016, *Astronomy and Computing*, 16, 17
- Tempel, E., Stoica, R. S., Martínez, V. J., et al. 2014a, *MNRAS*, 438, 3465
- Tempel, E., Tago, E., & Liivamägi, L. J. 2012, *A&A*, 540, A106
- Tempel, E., Tamm, A., Gramann, M., et al. 2014b, *A&A*, 566, A1
- Tremonti, C. A., Heckman, T. M., Kauffmann, G., et al. 2004, *ApJ*, 613, 898
- Werner, S. V., Hatch, N., Muzzin, A., et al. 2021, in *Galaxy Cluster Formation II*, 20
- Yasuda, N., Fukugita, M., Narayanan, V. K., et al. 2001, *AJ*, 122, 1104
- Yun, K., Pillepich, A., Zinger, E., et al. 2019, *MNRAS*, 483, 1042
- Zeldovich, I. B., Einasto, J., & Shandarin, S. F. 1982, *Nature*, 300, 407

Appendix A: The properties of galaxies in poor and rich groups and single galaxies in low- and high-global-density environments

Tables A.1 - A.6 present median values of the morphological properties of VO and YS galaxies for single galaxies, satellites, and BGGs of LLGs in various global density environments. We also give the KS test p -values, which show the statistical significance of the differences between distributions for watershed regions ($D8 < 1$) and other global luminosity–density regions.

Table A.1. Median values of the galaxy properties, and the KS test p -values for VO single galaxies in various global density environments

(1)	(2)	(3)	(4)	(5)	(6)	(7)	(8)	(9)	(10)	(11)	(12)
$D8$	N_{gal}	M_{med}^*	p	σ_{med}^*	p	C_{med}	p	$D_n(4000)_{\text{med}}$	p	SFR_{med}	p
0 – 1	2797	10.69		157		0.35		1.88		-1.30	
1 – 2	3757	10.73	< 0.001	161	< 0.001	0.34	< 0.001	1.88	0.121	-1.26	< 0.001
2 – 3	2100	10.73	< 0.001	163	< 0.001	0.34	< 0.001	1.89	0.001	-1.28	0.005
3 – 4	1086	10.73	< 0.001	161	0.018	0.34	< 0.001	1.89	0.230	-1.28	0.124
4 – 5	570	10.74	< 0.001	164	0.008	0.34	< 0.001	1.90	0.017	-1.26	0.030
> 5	870	10.72	< 0.001	161	0.009	0.34	0.003	1.89	0.122	-1.29	0.300

Notes. Columns are as follows: (1): Global luminosity–density $D8$ range; (2): Number of galaxies in corresponding global luminosity–density range; (3–4): Median value of the stellar mass, M_{med}^* , and p -value of the KS test between a given population in the lowest global density environment ($D8 \leq 1$) and in the given global density interval; (5–6): Median value of the stellar velocity dispersion σ^* and p -value of the KS test as in column (3); (7–8): Median value of the concentration index C and p -value of the KS test as in column (3); (9–10): Median value of the $D_n(4000)$ index, $D_n(4000)_{\text{med}}$, and p -value of the KS test as in column (3); (11–12): Median value of the star formation rate, SFR_{med} , and p -value of the KS test as in column (3).

Table A.2. Median values of the galaxy properties, and the KS test p -values for VO satellite galaxies in LLGs in various global density environments

(1)	(2)	(3)	(4)	(5)	(6)	(7)	(8)	(9)	(10)	(11)	(12)
$D8$	N_{gal}	M_{med}^*	p	σ_{med}^*	p	C_{med}	p	$D_n(4000)_{\text{med}}$	p	SFR_{med}	p
0 – 1	595	10.61		151		0.35		1.88		-1.39	
1 – 2	2069	10.64	< 0.001	155	0.040	0.35	< 0.001	1.89	0.108	-1.33	0.02
2 – 3	1732	10.65	< 0.001	156	0.001	0.34	< 0.001	1.89	< 0.001	-1.35	0.32
3 – 4	1173	10.63	< 0.001	155	0.018	0.35	< 0.001	1.89	0.010	-1.36	0.18
4 – 5	650	10.64	< 0.001	159	0.001	0.35	< 0.001	1.89	0.005	-1.35	0.20
> 5	1076	10.64	< 0.001	155	0.004	0.35	0.003	1.89	0.007	-1.34	0.10

Notes. Columns are as follows: (1): Global luminosity–density $D8$ range; (2): Number of galaxies in corresponding global luminosity–density range; (3–4): Median value of the stellar mass, M_{med}^* , and p -value of the KS test between a given population in the lowest global density environment ($D8 \leq 1$) and in the given global density interval; (5–6): Median value of the stellar velocity dispersion σ^* and p -value of the KS test as in column (3); (7–8): Median value of the concentration index C and p -value of the KS test as in column (3); (9–10): Median value of the $D_n(4000)$ index, $D_n(4000)_{\text{med}}$, and p -value of the KS test as in column (3); (11–12): Median value of the star formation rate, SFR_{med} , and p -value of the KS test as in column (3).

Table A.3. Median values of the galaxy properties, and the KS test p -values for VO BGGs in LLGs in various global density environments

(1)	(2)	(3)	(4)	(5)	(6)	(7)	(8)	(9)	(10)	(11)	(12)
$D8$	N_{gal}	M_{med}^*	p	σ_{med}^*	p	C_{med}	p	$D_n(4000)_{\text{med}}$	p	SFR_{med}	p
0 – 1	770	10.90		182		0.33		1.90		-1.21	
1 – 2	2042	10.97	< 0.001	190	0.098	0.33	< 0.001	1.92	0.053	-1.16	< 0.001
2 – 3	1465	10.99	< 0.001	195	0.025	0.33	< 0.001	1.93	< 0.001	-1.16	0.002
3 – 4	963	10.98	< 0.001	198	< 0.001	0.32	< 0.001	1.92	0.001	-1.17	0.013
4 – 5	498	10.98	< 0.001	194	0.074	0.32	< 0.001	1.93	< 0.001	-1.16	0.002
> 5	797	10.98	< 0.001	193	0.20	0.33	0.003	1.93	< 0.001	-1.16	0.006

Notes. Columns are as follows: (1): Global luminosity–density $D8$ range; (2): Number of galaxies in corresponding global luminosity–density range; (3–4): Median value of the stellar mass, M_{med}^* , and p -value of the KS test between a given population in the lowest global density environment ($D8 \leq 1$) and in the given global density interval; (5–6): Median value of the stellar velocity dispersion σ^* and p -value of the KS test as in column (3); (7–8): Median value of the concentration index C and p -value of the KS test as in column (3); (9–10): Median value of the $D_n(4000)$ index, $D_n(4000)_{\text{med}}$, and p -value of the KS test as in column (3); (11–12): Median value of the star formation rate, SFR_{med} , and p -value of the KS test as in column (3).

Table A.4. Median values of the galaxy properties, and the KS test p -values for YS single galaxies with $D_n(4000) < 1.75$ in various global density environments

(1)	(2)	(3)	(4)	(5)	(6)	(7)	(8)	(9)	(10)	(11)	(12)
$D8$	N_{gal}	M_{med}^*	p	σ_{med}^*	p	C_{med}	p	$D_n(4000)_{\text{med}}$	p	SFR_{med}	p
0 – 1	7425	10.38		84		0.42		1.39		0.21	
1 – 2	8222	10.41	< 0.001	88	0.01	0.42	0.03	1.40	< 0.001	0.20	0.720
2 – 3	4098	10.42	< 0.001	89	< 0.001	0.42	0.05	1.41	< 0.001	0.19	0.157
3 – 4	2054	10.42	< 0.001	91	< 0.001	0.42	0.31	1.41	< 0.001	0.19	0.103
4 – 5	997	10.41	0.005	89	0.013	0.42	0.04	1.41	< 0.001	0.18	0.071
> 5	1459	10.41	< 0.001	89	0.001	0.42	0.15	1.41	< 0.001	0.19	0.002

Notes. Columns are as follows: (1): Global luminosity–density $D8$ range; (2): Number of galaxies in corresponding global luminosity–density range; (3–4): Median value of the stellar mass, M_{med}^* , and p -value of the KS test between a given population in the lowest global density environment ($D8 \leq 1$) and in the given global density interval; (5–6): Median value of the stellar velocity dispersion σ^* and p -value of the KS test as in column (3); (7–8): Median value of the concentration index C and p -value of the KS test as in column (3); (9–10): Median value of the $D_n(4000)$ index, $D_n(4000)_{\text{med}}$, and p -value of the KS test as in column (3); (11–12): Median value of the star formation rate, SFR_{med} , and p -value of the KS test as in column (3).

Table A.5. Median values of the galaxy properties, and the KS test p -values for YS satellite galaxies in LLGs in various global density environments

(1)	(2)	(3)	(4)	(5)	(6)	(7)	(8)	(9)	(10)	(11)	(12)
$D8$	N_{gal}	M_{med}^*	p	σ_{med}^*	p	C_{med}	p	$D_n(4000)_{\text{med}}$	p	SFR_{med}	p
0 – 1	1392	10.34		84		0.42		1.37		0.166	
1 – 2	3539	10.37	0.002	88	0.01	0.42	0.37	1.40	< 0.001	0.150	0.526
2 – 3	2611	10.40	< 0.001	89	< 0.001	0.42	0.65	1.42	< 0.001	0.125	0.014
3 – 4	1797	10.41	< 0.001	91	< 0.001	0.41	0.01	1.44	< 0.001	0.111	0.001
4 – 5	905	10.39	0.002	89	0.013	0.41	0.01	1.42	< 0.001	0.105	0.010
> 5	1460	10.49	< 0.001	89	0.001	0.42	0.64	1.42	< 0.001	0.125	0.152

Notes. Columns are as follows: (1): Global luminosity–density $D8$ range; (2): Number of galaxies in corresponding global luminosity–density range; (3–4): Median value of the stellar mass, M_{med}^* , and p -value of the KS test between a given population in the lowest global density environment ($D8 \leq 1$) and in the given global density interval; (5–6): Median value of the stellar velocity dispersion σ^* and p -value of the KS test as in column (3); (7–8): Median value of the concentration index C and p -value of the KS test as in column (3); (9–10): Median value of the $D_n(4000)$ index, $D_n(4000)_{\text{med}}$, and p -value of the KS test as in column (3); (11–12): Median value of the star formation rate, SFR_{med} , and p -value of the KS test as in column (3).

Table A.6. Median values of the galaxy properties, and the KS test p -values for YS BGGs in LLGs in various global density environments

(1)	(2)	(3)	(4)	(5)	(6)	(7)	(8)	(9)	(10)	(11)	(12)
$D8$	N_{gal}	M_{med}^*	p	σ_{med}^*	p	C_{med}	p	$D_n(4000)_{\text{med}}$	p	SFR_{med}	p
0 – 1	1043	10.60		102		0.42		1.42		0.352	
1 – 2	1806	10.67	< 0.001	109	< 0.001	0.41	< 0.001	1.45	0.013	0.359	0.180
2 – 3	1132	10.70	< 0.001	111	< 0.001	0.41	< 0.001	1.47	< 0.001	0.343	0.655
3 – 4	672	10.69	< 0.001	112	< 0.001	0.40	< 0.001	1.48	< 0.001	0.290	0.010
4 – 5	373	10.67	< 0.001	111	0.003	0.41	0 – 93	1.49	< 0.001	0.303	0.15
> 5	559	10.66	0.004	106	0.061	0.41	0.010	1.47	< 0.001	0.299	0.010

Notes. Columns are as follows: (1): Global luminosity–density $D8$ range; (2): Number of galaxies in corresponding global luminosity–density range; (3–4): Median value of the stellar mass, M_{med}^* , and p -value of the KS test between a given population in the lowest global density environment ($D8 \leq 1$) and in the given global density interval; (5–6): Median value of the stellar velocity dispersion σ^* and p -value of the KS test as in column (3); (7–8): Median value of the concentration index C and p -value of the KS test as in column (3); (9–10): Median value of the $D_n(4000)$ index, $D_n(4000)_{\text{med}}$, and p -value of the KS test as in column (3); (11–12): Median value of the star formation rate, SFR_{med} , and p -value of the KS test as in column (3).